MOLECULAR AND CELLULAR BIOLOGY, Oct. 2010, p. 4901–4921 Vol. 30, No. 20
0270-7306/10/$12.00 doi:10.1128/MCB.00409-10

Mechanism of Hypoxia-Induced NF-κB▽†

Carolyn Culver,[1] Anders Sundqvist,[2] Sharon Mudie,[1] Andrew Melvin,[1] Dimitris Xirodimas,[1] and Sonia Rocha[1]*

College of Life Sciences, Wellcome Trust Centre for Gene Regulation and Expression, MSI/WTB/JBC Complex, Dow Street, University of Dundee, Dundee DD1 5EH, Scotland,[1] and Ludwig Institute for Cancer Research, Uppsala University, S-751 24 Uppsala, Sweden[2]

Received 8 April 2010/Returned for modification 1 June 2010/Accepted 13 July 2010

NF-κB activation is a critical component in the transcriptional response to hypoxia. However, the underlying mechanisms that control its activity under these conditions are unknown. Here we report that under hypoxic conditions, IκB kinase (IKK) activity is induced through a calcium/calmodulin-dependent kinase 2 (CaMK2)-dependent pathway distinct from that for other common inducers of NF-κB. This process still requires IKK and the IKK kinase TAK1, like that for inflammatory inducers of NF-κB, but the TAK1-associated proteins TAB1 and TAB2 are not essential. IKK complex activation following hypoxia requires Ubc13 but not the recently identified LUBAC (linear ubiquitin chain assembly complex) ubiquitin conjugation system. In contrast to the action of other NF-κB inducers, IKK-mediated phosphorylation of IκBα does not result in its degradation. We show that this results from IκBα sumoylation by Sumo-2/3 on critical lysine residues, normally required for K-48-linked polyubiquitination. Furthermore, inhibition of specific Sumo proteases is sufficient to release RelA from IκBα and activate NF-κB target genes. These results define a novel pathway regulating NF-κB activation, important to its physiological role in human health and disease.

Exposure to hypoxia, or lack of oxygen, initiates a myriad of cellular and molecular responses, which are required for the cell to adapt to the environment of inadequate oxygen (19, 31). The heterodimeric transcription factor HIF (hypoxia-inducible factor) has emerged as the master regulator of this complex cellular response (reviewed in reference 36). The dimers consist of one of three oxygen-sensitive α subunits (HIF-1α to HIF-3α) coupled with the constitutively expressed β subunit, HIF-1β. Under normoxic conditions, HIF-α subunits have an extremely short half-life and a low level of transcriptional activity due to the combined action of a class of prolyl hydroxylase domain (PHD) enzymes and the factor inhibiting HIF (FIH) (13, 17). PHD enzymes hydroxylate the HIF-α subunits, which promotes the binding of von Hippel-Lindau protein, an E3 ligase complex, leading to the targeting of HIF-1α for proteasomal degradation (13, 17). FIH negatively regulates HIF-1α through its action as an asparaginyl hydroxylase, which results in the suppression of HIF-1α transcriptional activity (reviewed in reference 17). However, HIF does not mediate the cellular response to hypoxia independently. A number of additional transcription factors have been shown to be responsive to hypoxia; among these is the major transcription factor NF-κB (10, 19).

NF-κB is a family of seven proteins, including RelA (p65), RelB, c-Rel, NF-κB1 (p105/p50), and NF-κB2 (p100/p52), which are encoded on five different genes (reviewed in a special edition of *Oncogene* [15]). Therefore, there are many possible combinations of homo- and heterodimers that act to modulate NF-κB DNA binding activity; however, the p50/RelA heterodimer is the most commonly studied. In most cell types, NF-κB is held inactive in the cytoplasm by specific binding to a member of the IκB family of inhibitory proteins, including IκBα, -β, and -ε. NF-κB activation occurs in response to a large range of external stimuli, including inflammatory cytokines, such as tumor necrosis factor α (TNF-α); bacterial components, such as lipopolysaccharide (LPS); and viral infection (reviewed in reference 27). These activate one of two major pathways leading to NF-κB activation: the canonical or the noncanonical pathway (35). Activation via the canonical pathway occurs when an external ligand binds to a specific membrane-bound receptor, resulting in oligomerization, recruitment of a number of adaptor molecules, and ubiquitin-dependent activation of the TAK1–IκB kinase (IKK) complex (1). IKK mediates the phosphorylation of IκBα at Ser32 and Ser36, which targets IκBα for proteasomal degradation, culminating in the translocation of NF-κB to the nucleus. In the noncanonical pathway, ligand binding results in the activation of NF-κB-inducing kinase (NIK) and the consequent activation of IKKα, leading to the processing of p100 and the translocation of p52/RelB into the nucleus (35).

Importantly, aberrant activation of NF-κB, which involves its constitutive localization in the nucleus, is associated with many diseases (29, 30). Since NF-κB both is activated by and induces the expression of cytokines and chemokines, it is associated with many inflammatory diseases, such as arthritis, inflammatory bowel disease, and asthma (reviewed in reference 15). In addition, NF-κB is a regulator of proliferation, apoptosis, angiogenesis, and metastasis (15, 16). HIF is also known to contribute to tumorigenesis through the regulation of metastasis, angiogenesis, metabolism, proliferation, and response to radiation therapy (reviewed in reference 14). Given the parallels between these two major transcription factors, it is perhaps

* Corresponding author. Mailing address: College of Life Sciences, Wellcome Trust Centre for Gene Regulation and Expression, MSI/WTB/JBC Complex, Dow Street, University of Dundee, Dundee DD1 5EH, Scotland. Phone: 44 1382 385 792. Fax: 44 1382 388 675. E-mail: s.rocha@dundee.ac.uk.

▽ Published ahead of print on 9 August 2010.

† The authors have paid a fee to allow immediate free access to this article.

surprising that so few mechanistic data exist regarding how hypoxic stimuli may modulate NF-κB activity.

The seminal discovery that hypoxia can induce the activation of NF-κB was made in 1994 (22). In those early studies, it was reported that hypoxia-induced NF-κB was mediated by phosphorylation at a tyrosine residue on IκBα and that this activation did not result in IκB degradation, suggesting an IKK-independent mechanism. Despite these exciting early discoveries and subsequent reports from a number of independent laboratories demonstrating that NF-κB is an important contributor to the hypoxic response (10, 19), the mechanism underlying this activation remains undefined.

Here we demonstrate the crucial roles of the IKK complex and calcium/calmodulin-dependent kinase 2 (CaMK2) in this activation, and we report, to our knowledge for the first time, the role of TAK1 as a key upstream IKK kinase required for the hypoxic activation of NF-κB. We also reveal the requirement of the Ubc13 ubiquitin-conjugating system for the activation of both TAK1 and IKK, and in addition we find that hypoxia-induced NF-κB both activates and represses specific target genes, which contribute to the cellular response to hypoxia. Interestingly, we demonstrate that the lack of IκBα degradation following hypoxia is due to sumoylation of key ubiquitin-accepting lysine residues by Sumo-2/3. Importantly, we show that modulation of Sumo-2/3 conjugation/deconjugation has a direct impact on NF-κB activity.

MATERIALS AND METHODS

Cells. Human osteosarcoma cells (U2OS), human breast cancer cells (MDA-MB-231), human embryonic kidney cells (HEK293), and wild-type, IKKα-null, IKKβ-null, IKKα/β-null, IKKγ-null, TAK1-null, TAB1-null, TAB2-null, TRAF2-null, and TRAF6-null mouse embryonic fibroblasts (MEFs) were maintained under 5% CO_2 in Dulbecco's modified Eagle's medium (DMEM; Lonza) supplemented with 10% fetal bovine serum (FBS) (Invitrogen), 1% penicillin-streptomycin (Lonza), and 1% L-glutamine (Lonza). Normal human breast epithelial cells (MCF10A) were maintained in DMEM–Ham's F-12 nutrient mixture with 5% FBS (Invitrogen), 1% penicillin-streptomycin, and 1% L-glutamine, supplemented with 10 μg/ml insulin (Sigma), 20 ng/ml epidermal growth factor (EGF; Sigma), and 5 μg/ml hydrocortisone (Sigma). Primary mouse endothelial cells (MEC) were maintained in MCBD-131 (Invitrogen) with 10% FBS, 1% penicillin-streptomycin, and 1% L-glutamine. These cells were grown in 0.2% gelatin (Sigma)-coated dishes. U2OS, HEK293, and MDA-MB-231 cells were obtained from the European Collection of Cell Cultures (ECACC). IKKα-, IKKβ-, and IKKα/β-null MEFs were a kind gift from I. Verma (San Diego, CA); TAK1- and TAB2-null MEFs were a kind gift from S. Akira (Tokyo, Japan); TAB1-null MEFs were a kind gift from S. Gosh (San Diego, CA); ATM (ataxia telangiectasia mutated) mutant and ATM-reconstituted cells were a gift from C. Smythe (Sheffield, United Kingdom) and have been described previously (32); and PRKR-like endoplasmic reticulum kinase (PERK) wild-type and PERK-null MEFs were a gift from D. Ron (New York, NY). TRAF2- and TRAF6-null cells were a gift from T. Mak (Toronto, Canada). IKKγ-null cells were a gift from M. Pasparakis (Cologne, Germany). MCF10A cells were a kind gift from A. Schulze (CRUK, London, United Kingdom), and MEC were a gift from M. Soares (GIS, Oeiras, Portugal).

Plasmids. The 3×κB-ConA luciferase, concanavalin A (ConA)-luciferase, and BcL-x_L constructs have been described previously (32). The RSV-IκBα wild-type construct was a gift from N. Perkins (Dundee, United Kingdom). Interleukin 8 (IL-8) luciferase constructs were a kind gift from M. Krascht (Hannover, Germany). PTEN-luciferase constructs were a kind gift from V. Rangnekar (Lexington, KY). The HIF-1α expression plasmid was a gift from C. Bracken (Adelaide, Australia). pSilencer (Ambion) short hairpin RNA (shRNA) constructs were created according to the manufacturer's instructions. His_6-ubiquitin, His_6-NEDD8, His_6-Sumo-2, His_6-Sumo-3, pCDNA3-Senp1, pCDNA3-Senp2, RSV-IκBα Lys21A, and RSV-IκBα Tyr42A were a kind gift from R. Hay (Dundee, United Kingdom). The glutathione *S*-transferase (GST)-TAK1/TAB1 fusion construct was a kind gift from P. Cohen (Dundee, United Kingdom), and the pCMV6-CAMK2δ construct was obtained from Origene.

Inhibitors and chemicals. The IKK inhibitor BAY 11-7082, the CaMK inhibitor KN-93, thapsigargin, and MG132 were purchased from Merck Biosciences. H_2O_2 was purchased from Sigma. Pervanadate was made fresh from a solution containing H_2O_2 and sodium orthovanadate (Sigma). 5Z-7-oxozeaenol was a kind gift from P. Cohen (Dundee, United Kingdom).

Chromatin immunoprecipitation (ChIP). Cells were grown to 70% confluence and were cross-linked with 1% formaldehyde at room temperature for 10 min. Glycine was added to a final concentration of 0.125 M for 5 min at room temperature. Cells were washed twice with 10 ml of ice-cold phosphate-buffered saline (PBS) and were then scraped into 2 ml ice-cold harvest buffer (PBS, 1 mM phenylmethylsulfonyl fluoride [PMSF], 1 μg/ml leupeptin, 1 μg/ml aprotinin) before being centrifuged at 1,000 rpm in an Avanti benchtop centrifuge at 4°C for 10 min. The supernatant was removed, and the pellet was resuspended in 0.5 ml of lysis buffer (1% sodium dodecyl sulfate [SDS], 10 mM EDTA, 50 mM Tris-HCl [pH 8.1], 1 mM PMSF, 1 μg/ml leupeptin, 1 μg/ml aprotinin) and then left on ice for 10 min. Samples were then sonicated at 4°C seven times. Each sonication was carried out for 20 s, with a 1-min gap between sonications. Supernatants were recovered by centrifugation at 12,000 rpm in an Eppendorf microcentrifuge for 10 min at 4°C before being diluted 10-fold in dilution buffer (1% Triton X-100, 2 mM EDTA, 150 mM NaCl, 20 mM Tris-HCl [pH 8.1]). Samples were then precleared for 2 h at 4°C with 2 μg of sheared salmon sperm DNA and 20 μl of protein A-Sepharose (50% slurry). At this stage, 10% of the material was kept and stored at −20°C as input material. Immunoprecipitations were performed overnight with specific antibodies (2 μg), with the addition of Brij 35 detergent to a final concentration of 0.1%. The immune complexes were captured by incubation with 30 μl of protein A-Sepharose (50% slurry) and 2 μg salmon sperm DNA for 1 h at 4°C. The immunoprecipitates were washed sequentially for 5 min each at 4°C in wash buffer 1 (0.1% SDS, 1% Triton X-100, 2 mM EDTA, 20 mM Tris-HCl [pH 8.1], 150 mM NaCl), wash buffer 2 (0.1% SDS, 1% Triton X-100, 2 mM EDTA, 20 mM Tris-HCl [pH 8.1], 500 mM NaCl), and wash buffer 3 (0.25 M LiCl, 1% Nonidet P-40, 1% deoxycholate, 1 mM EDTA, 10 mM Tris-HCl [pH 8.1]). Beads were washed twice with Tris-EDTA (TE) buffer and were eluted with 100 μl of elution buffer (1% SDS, 0.1 M $NaHCO_3$). Eluates were purified using a PCR purification kit (Qiagen).

Quantitative PCR (qPCR) analysis. Total RNA was extracted with the NucleoSpin RNA II isolation system (catalog no. 740955; Macherey-Nagel) or an Invisorb spin cell RNA kit (Invitek) according to the manufacturer's directions. RNA was converted to cDNA using a Quantitect reverse transcription kit (Qiagen). cDNA was used in semiquantitative PCR. For quantitative PCR, a Brilliant II Sybr green kit (Stratagene/Agilent) was used, and samples were analyzed using an Mx3005P QPCR machine (Stratagene/Agilent). Actin was used as a normalizing gene in all experiments.

Antibodies. The following antibodies were used: anti-HIF-1α (MAB1536; R&D Systems), anti-HIF-1β (3718; Cell Signaling), polyclonal anti-p52 (sc-848; Santa Cruz), anti-RelA (sc-372; Santa Cruz), anti-PCNA (P8825; Sigma), anti-IKKα/β (sc-7607; Santa Cruz), anti-β-actin (A5441; Sigma), anti-TRAF6 (sc-8609; Santa Cruz), anti-TAK1 (4505; Cell Signaling), anti-IκBα (sc-371 [Santa Cruz] and 4812 [Cell Signaling]), anti-TRAF2 (AP1004; Merck Biosciences), anti-phospho-eIF2α Ser51 (9721; Cell Signaling), anti-eIF2α (9722; Cell Signaling), anti-phospho-Tyr42 IκBα (ab24783; Abcam), anti-phospho-IκBα Ser32/36 (9246; Cell Signaling), anti-phospho-IKKα/β (2681; Cell Signaling), anti-acetyl histone H3 (06-599; Upstate Biotechnology), anti-Pol II (sc-47701; Santa Cruz), anti-PHD1 (A300-62A-2; Bethyl Laboratories), anti-PHD2 (ab4561; Abcam), anti-PHD3 (A300-327A; Bethyl Laboratories), anti-Ubc13 (4919; Cell Signaling), anti-UbcH5a, anti-Senp1, anti-Senp2, anti-Senp6, and anti-Senp7 (kind gifts from Ron Hay [Dundee, United Kingdom]), anti-HOIP (ab2919; Abcam), anti-HOIL-1L (ab38540; Abcam), anti-Senp5 (ab58420; Abcam), anti-IAP2 (3130; Cell Signaling), anti-PTEN (9559; Cell Signaling), antiphosphotyrosine (9411; Cell Signaling), anti-TAB1 (3225; Cell Signaling), and anti-pan-CaMK2 (3362; Cell Signaling).

siRNA. Small interfering RNA (siRNA) duplex oligonucleotides were synthesized by MWG and were transfected using INTERFERin (Polyplus) according to the manufacturer's instructions. In brief, cells were plated the day before transfection at a concentration of 2×10^5 per well in 6-well plates. The following day, cells were transfected with siRNA oligonucleotides at a final concentration of 5 nM in fresh medium (final volume, 2.2 ml). Cells were incubated for an additional 48 h prior to harvest. Hypoxic stress treatments were performed within the 48-h posttransfection window.

Hypoxia induction. Cells were incubated in varying O_2 levels in an InVivo 300 hypoxia workstation (Ruskinn, United Kingdom). For short hypoxia exposures (less than 60 min), the medium was replaced with a hypoxia-equilibrated medium

(the medium was equilibrated in the hypoxia workstation for 30 min before being added to the cells). Cells were lysed for extraction of protein and RNA in the workstation to avoid reoxygenation.

Oligonucleotide sequences. (i) RT-PCR. The primers used for reverse transcription-PCR (RT-PCR) of human genes were as follows: for actin, CTGGG AGTGGGTGGAGGC (forward) and TCAACTGGTCTCAAGTCAGTG (reverse); for IL-8, CCAGGAAGAAACCACCGGA (forward) and GAAATCAG GAAGGCTGCCAAG (reverse); for PTEN, CGGTGTCATAATGTCTTT CAGC (forward) and TGAAGGCGTATACAGGAACAAT (reverse); for XIAP, CTGTTAAAAGTCATCTTCTCTTGAAA (forward) and GACCCTCC CCTTGGACC (reverse); for IAP2, GTCAAATGTTGAAAAAGTGCCA (forward) and GGGAAGAGGAGAGAGAAAGAGC (reverse); for CAMKIIδ, GGAATTTCTCAGCAGCCAAG (forward) and AGTAAGGCCTGGGTCA CAGA (reverse); for RelA, CTGCCGGGATGGCTTCTAT (forward) and CC GCTTCTTCACACACTGGAT (reverse); for p100, AGCCTGGTAGACACG TACCG (forward) and CCGTACGCACTGTCTTCCTT (reverse); and for SENP3, TCGCCTCACATCAACAGAGA (forward) and GGTGAAAAGGTG GACCAAAA (reverse).

The primers used for RT-PCR of mouse genes were as follows: for mActin, ATGCTCCCCGGGCTGTAT (forward) and CATAGGAGTCCTTCTGACCC ATTC (reverse); for mCXCL1, TCTCCGTTACTTGGGGACAC (forward) and CCACACTCAAGAATGGTCGC (reverse); for mCXCL2, CTTTGGTTCTTC CGTTGAGG (forward) and CAAAAAGTTTGCCTTGACCC (reverse); and for mIκBα, GTCTCCCTTCACCTGACCAA (forward) and CAGCAGCTCAC GGAGGAC (reverse).

(ii) ChIP PCR. The primers used for ChIP PCR were as follows: for the IL-8 promoter, AAGAAAACTTTCGTCATACTCCG (forward) and TGGCTTTTT ATATCATCACCCTAC (reverse); for the IL-8 control region, ATCATGGGT CCTCAGAGGTCAGAC (forward) and GGTGGGAGGGAGGTGTTATCT AATG (reverse); for the PTEN promoter, CACCATGAGGACACAGATTT GGGG (forward) and GTGTAGAGGGAAATGCAGGGACGG (reverse); and for the PTEN control region, TGTATCCTTCCACCTCCTTTTGAAC (forward) and GGATCGCCCGGGGCCAGGCTCCGCG (reverse).

(iii) siRNA. The following siRNA oligonucleotides were used: control, CAGUC GCGUUUGCGACUGG; TAK1, UGGCUUAUCUUACACUGGA; RelA/p65, GCCCUAUCCCUUUACGUCA (1) and GCUGAUGUGCACCGACAAG (2); p100/p52, GAUGAAGAUUGAGCGGCCU (1) and CAGCCUAAGCAGAGA GGCU (2); CAMK2δ, UCAAGGCUGGAGCUUAUGA; Ubc13, GGCUAU AUGCCAUGAAUAA; UbcH5a, GAGAAUGGACUCAGAAAUA; HOIP, GCCUGCUAUUGCAGAAUAC; HOIL-1L, AGAUCGUGGUACAGAA GAA; HIF-1α, CUGAUGACCAGCAACUUGA; PHD1, GACUAUAUCG UGCCCUGCAUG; PHD2, GACGAAAGCCAUGGUUGCUUG; PHD3, GUCUAAGGCAAUGGUGGCUUG; SENP1, AGCUAUUACUCAGAU AAUC (a) and GUACAUGAUUCAGUAGAAC (b); SENP2, UUAUUCU GGUGCCUAUUCA (a) and AGAUCAGAGUGACAGUUAC (b); SENP3, ACGUGGACAUCUUCAAUAA (a) and GCAUAUUGCCAAGUAUCUA (b); SENP5, AGAAGUCCUUGGAAGAUUA (a) and UAUGUAUGGUG AGCUGAUA (b); SENP6, UUAAUCCUGUAAGGUUAAG (a) and UCU GCUCAGUGUGGAUGAA (b); and SENP7, UGAGUUGAAUACCAU AGAA (a) and GAAGGACCUGUUGAACAUA (b).

(iv) shRNA. Control and HIF-1α shRNA sequences have been described previously (18). In addition, the following shRNA oligonucleotides were used: PHD1 sense, GATCCCCACATTGCTGCATGGTAGAATTCAAGAG ATTCTACCATGCAGCAATGTTTTTTGGAAA; PHD1 antisense, AGCTT TTCCAAAAAACATTGCTGCATGGTAGAATCTCTTGAATTCTACCAT GCAGCAATGTGGG; PHD2 sense, CATCCCCGTACAACCAGCATATG CTATTCAAGAGATAGCATATGCTGGTTGTACTTTTTGGAAA; PHD2 antisense, AGCTTTTCCAAAAAGTACAACCAGCATATGCTATCTCTT GAATAGCATATGCTGGTTGTACGGG; PHD3 sense, GATCCCCTAAG ACATGTCACCATTAATTCAAGAGATTAATGGTGACATGTCTTATTT TTGGAAA; and PHD3 antisense, AGCTTTTCCAAAAATAAGACATGT CACCATTAATCTCTTGAATTAATGGTGACATGTCTTAGGG.

Western blotting. Western blotting was performed essentially as described previously (32). Assays analyzing cytoplasmic proteins used 30 to 40 μg of protein, while analysis of nuclear proteins used 20 μg of protein. Analysis of whole-cell lysates used 20 to 30 μg of protein.

Statistical analysis. Analysis of variance (ANOVA) and Student *t* tests were performed on the means, and *P* values were calculated.

Other experimental procedures. Whole-cell protein extracts, nuclear extracts, electrophoretic mobility shift assay (EMSA) analysis, and luciferase assays were performed as described previously (reference 33 and references therein). His tag purification of ubiquitinated, NEDDylated, or sumoylated proteins was performed as described previously (42).

RESULTS

Hypoxia induces NF-κB DNA binding activity. To examine the effects of hypoxic stimuli on NF-κB activation, we initially used the osteosarcoma cell line U2OS as our model system.

Western blots of U2OS whole-cell lysates exposed to 1% O_2 for different lengths of time were evaluated for HIF-1α induction and activation of key NF-κB pathway components. All hypoxia treatments and lysate preparations were carried out in the InVivo 300 controlled-O_2 chamber; therefore, no reoxygenation events occurred in the course of experimentation. As expected, Western blot analysis demonstrated induction of HIF-1α following 30 min of hypoxia treatment (Fig. 1A). Hypoxia treatment also resulted in rapid and robust increases in both IKK (activation loop) and IκBα (Ser32/36) phosphorylation, which occurred with only 5 min of hypoxia exposure. These levels of induction were comparable to those observed upon treatment with TNF-α, a typical activator of this pathway. Interestingly, no degradation of IκBα could be detected with hypoxia treatment, while TNF-α treatment induced almost-total degradation of IκBα (Fig. 1A). Furthermore, hypoxia treatment resulted in IKK activation to levels very similar to those induced by the prototypical activator TNF-α in different cell lines, such as the breast carcinoma cell line MDA-MB-231 or the nontransformed breast epithelial cell line MCF10A (Fig. 1A), indicating that this was not a cell type-specific response.

To further characterize the response and sensitivity of the NF-κB pathway to hypoxia, cells were exposed to varying levels of O_2 for 60 min. Levels of O_2 ranged from moderate hypoxia (10% O_2) to more-severe hypoxia (3% O_2) and were compared to the normoxic control (~21% O_2). Cytoplasmic and nuclear extracts were prepared from cells subjected to these treatments and were analyzed by Western blotting to determine the activation of key components of the HIF and NF-κB signaling pathways (Fig. 1B). As expected, decreasing O_2 levels induced increased stabilization and nuclear accumulation of HIF-1α (Fig.1Ba). Moreover, IκBα phosphorylation (serines 32/36) was observed even in response to moderate hypoxia (5%) (Fig.1Bb). Importantly, hypoxic conditions resulted in increased nuclear accumulation of RelA, indicating that NF-κB is indeed activated and translocates in response to hypoxia (Fig.1Ba).

We investigated whether hypoxia also resulted in NF-κB DNA binding. The binding of NF-κB to a radiolabeled oligonucleotide containing the typical consensus sequence from the HIV long terminal repeat (LTR) was determined in response to 1% O_2 treatment for varying lengths of time (Fig. 1C). An oligonucleotide containing the consensus binding site for the OCT-1 transcription factor was used as a control. We observed rapid and sustained induction of NF-κB DNA binding activity in response to hypoxia. NF-κB DNA binding was induced as early as 30 min and continued through 60 h of exposure to 1% O_2. OCT-1 DNA binding was not severely affected by hypoxia treatment. In addition, no specific DNA binding was observed when we used an oligonucleotide with a mutated NF-κB binding site (Fig. 1D).

The sensitivity of this response was characterized using the same experimental conditions as for Fig. 1B, and nuclear extracts were evaluated for NF-κB DNA binding activity. As shown in Fig. 1E, not only was NF-κB DNA binding enhanced

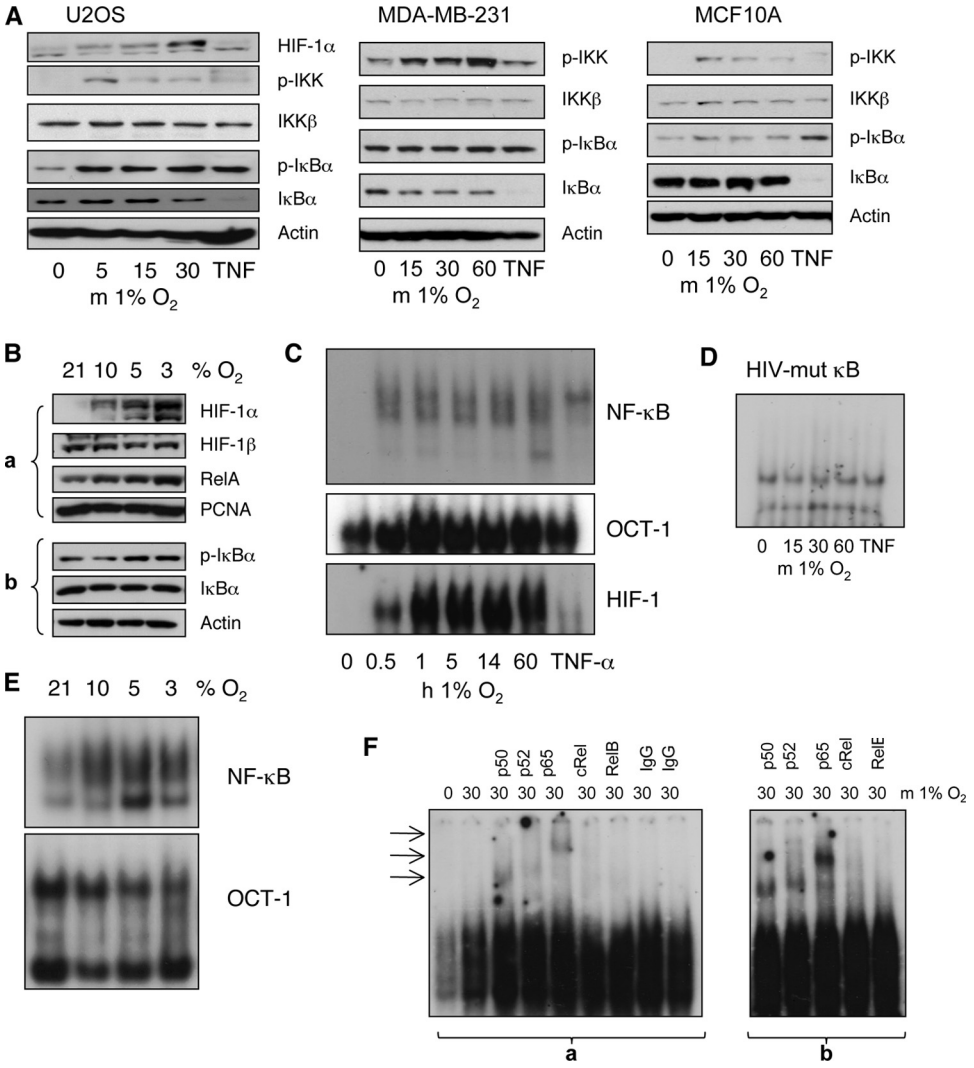

FIG. 1. Hypoxia induces NF-κB. (A) U2OS, MDA-MB-231, and MCF10A cells were exposed to 1% O_2 for the indicated times or were treated with 10 ng/ml TNF-α for 30 min prior to lysis. Whole-cell lysates were analyzed by Western blotting with the indicated antibodies. m, minutes. (B) U2OS cells were exposed for 60 min to decreasing concentrations of O_2 prior to harvest, and cytoplasmic/nuclear extracts were prepared. Nuclear (a) and cytoplasmic (b) extracts were analyzed as for panel A. (C) U2OS cells were exposed to 1% O_2 for different times before nuclear extracts were prepared and analyzed for the DNA binding activities of the indicated transcription factors. OCT-1 was used as a loading control. (D) U2OS cells were exposed to 1% O_2 or TNF-α for 30 min prior to nuclear extraction of proteins. Nuclear extracts were analyzed for DNA binding activity by using a radiolabeled oligonucleotide with a mutated NF-κB binding site (HIV-mut κB). (E) Nuclear extracts obtained under the same experimental conditions as the nuclear extracts analyzed in panel B were used in EMSA analysis for NF-κB and OCT-1 DNA binding. (F) Control nuclear extracts (0 min) and nuclear extracts exposed to 1% O_2 for 30 min were incubated with the indicated antibodies prior to being analyzed for DNA binding activity. Results of two representative experiments (a and b) are shown. Arrows indicate the shifted bands.

at lower O_2 levels, but it was also evident in response to very moderate hypoxia (10% O_2). To identify the NF-κB subunits that are activated by hypoxia, we performed supershift analysis using specific antibodies for the different NF-κBs. Antibodies directed against p50, p52, and RelA were able to supershift the complex (Fig. 1F). These data demonstrate that NF-κB activation occurs readily in response to even moderate fluctuations toward hypoxic conditions and coincides with other hallmarks of NF-κB activation, including IκBα phosphorylation.

Hypoxia-induced NF-κB is both an activator and a repressor of target genes. Since hypoxia induced NF-κB DNA binding and RelA nuclear accumulation, we investigated NF-κB transcriptional activity following this stimulus. Using a panel of validated NF-κB target gene promoters fused to a luciferase reporter, we investigated the effects of hypoxic stress on NF-κB-mediated promoter regulation. The NF-κB targets and luciferase constructs selected were Bcl-x_L, IL-8, and PTEN, and cells were exposed to 1% O_2 for 16 h (Fig. 2A). Bcl-x_L and IL-8 luciferase constructs were induced, while PTEN-luciferase was repressed. All of these responses were dependent on a functional NF-κB binding site; luciferase reporter constructs where the κB site was mutated or deleted were not responsive to hypoxia (Fig. 2A). This analysis suggests that hypoxia-induced NF-κB can activate and repress targets in a promoter-dependent manner. Interestingly, when an artificial luciferase reporter construct containing three copies of the consensus κB

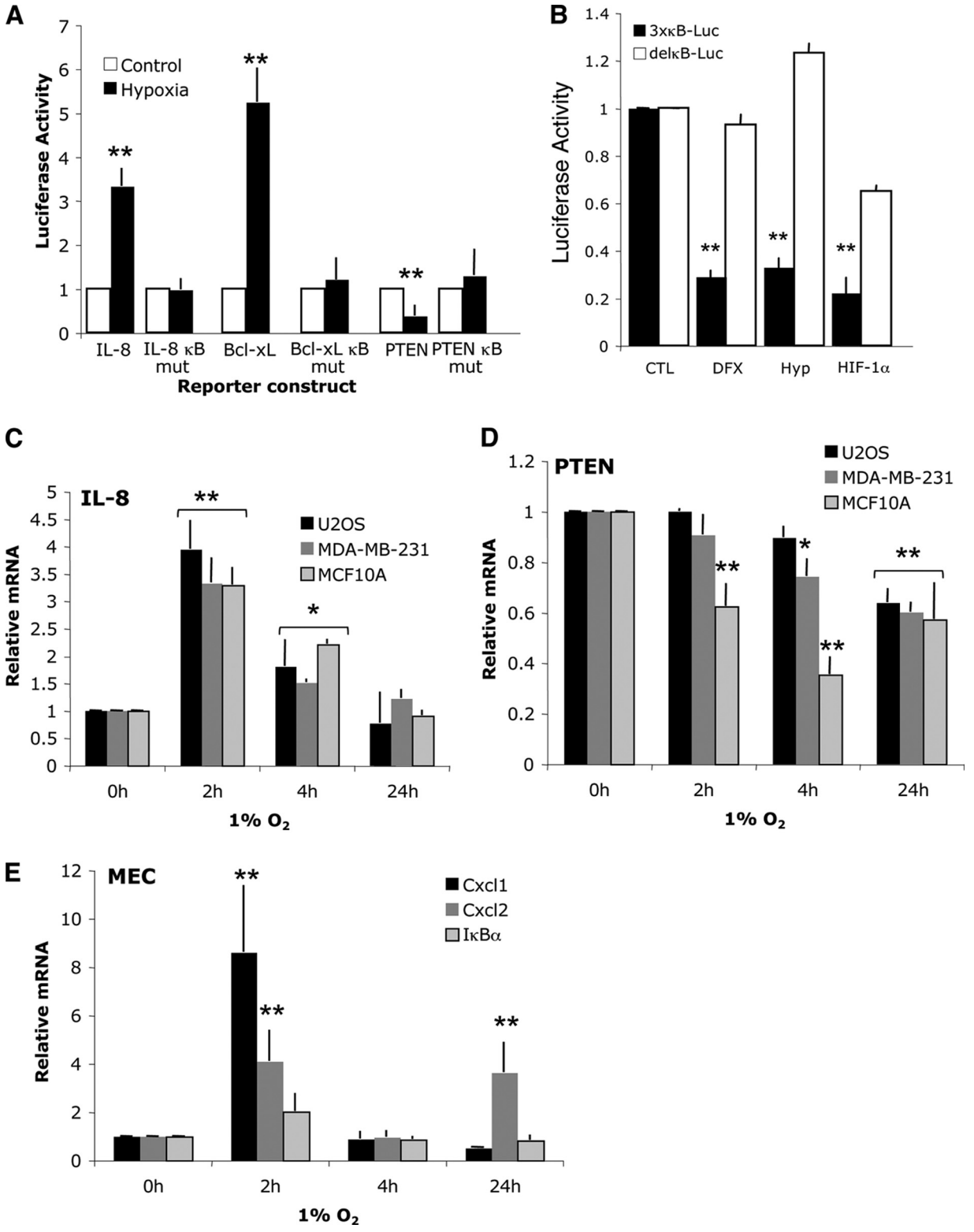

FIG. 2. Hypoxia modulates NF-κB to both activate and repress target genes. (A) U2OS cells were transfected with 1 μg of the indicated luciferase reporter constructs and were treated for 16 h with 1% O_2 prior to luciferase measurements. The graph depicts mean activation or repression relative to the luciferase activity of control samples, plus standard deviations. (B) U2OS cells were transfected with 1 μg of the 3×κB-ConA-luciferase or deleted-κB ConA-luciferase (delκB) construct. Cells either were cotransfected with 1 μg of an empty plasmid (CTL) or a HIF-1α expression plasmid or were treated with 1% O_2 (Hyp) or 100 μM DFX for 16 h prior to harvest and luciferase measurement. (C and D) U2OS, MDA-MB-231, and MCF10A cells were treated with 1% O_2 for the indicated times prior to harvest and mRNA extraction. IL-8 (C) and (D) PTEN mRNA levels were analyzed by quantitative PCR. Graphs depict IL-8 and PTEN mRNA levels compared to levels in untreated samples (0h). (E) Mouse endothelial cells were exposed to 1% O_2 for the indicated times prior to harvest and mRNA extraction. The indicated genes were analyzed by qPCR. *, $P \leq 0.050$; **, $P \leq 0.010$.

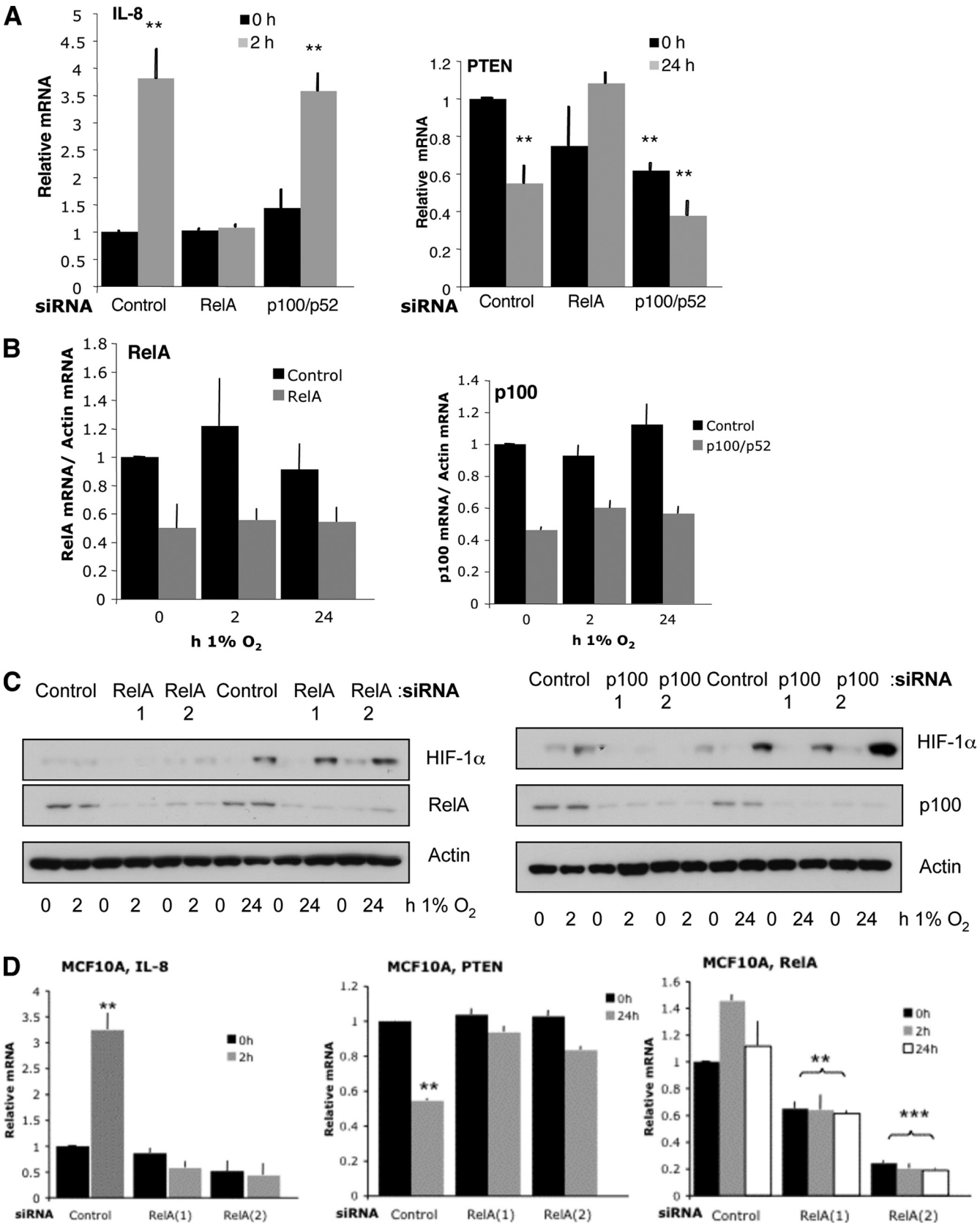

FIG. 3. Induction of IL-8 and repression of PTEN by hypoxia are RelA dependent. (A) U2OS cells were transfected with specific siRNA oligonucleotides prior to hypoxic stress exposure for the indicated times. IL-8 and PTEN mRNAs were analyzed by qPCR. (B) U2OS cells were treated and processed as for panel A, but qPCR was performed for RelA and p100 levels. (C) U2OS cells were transfected with specific siRNA oligonucleotides prior to hypoxic stress exposure for the indicated times. Whole-cell lysates were analyzed by Western blotting. (D) MCF10A cells were transfected with specific siRNA oligonucleotides prior to hypoxia exposure for the indicated times. IL-8 and PTEN mRNAs were analyzed by qPCR. *, $P \leq 0.050$; **, $P \leq 0.010$.

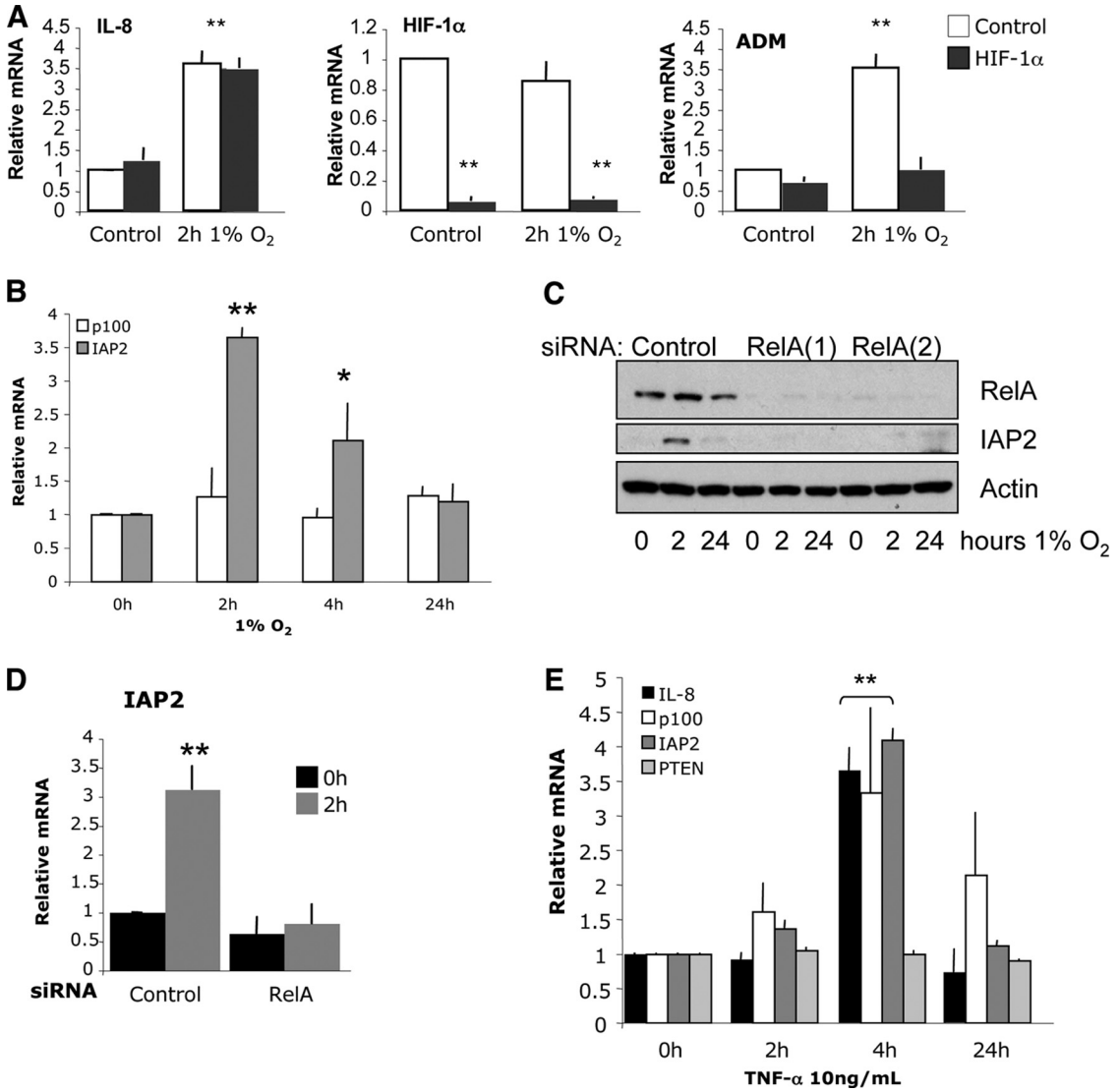

FIG. 4. NF-κB-mediated responses to hypoxia differ from those to TNF-α. (A) U2OS cells were transfected with HIF-1α siRNA oligonucleotides and were then exposed to hypoxia for 2 h prior to RNA extraction. HIF-1α, IL-8, and ADM mRNA levels were analyzed by qPCR. (B) U2OS cells were exposed to 1% O_2 for the indicated periods prior to RNA extraction. p100 and IAP2 mRNA levels were analyzed by qPCR. (C) U2OS cells were transfected with specific siRNA oligonucleotides prior to hypoxic stress exposure for the indicated times. Whole-cell lysates were analyzed by Western blotting. (D) U2OS cells were transfected with specific siRNA oligonucleotides prior to hypoxic stress exposure for the indicated times. IAP2 mRNA was analyzed by qPCR. (E) U2OS cells were treated with 10 ng/ml TNF-α for the indicated periods prior to RNA extraction. IL-8, p100, IAP2, and PTEN mRNA levels were analyzed by qPCR. *, $P \leq 0.050$; **, $P \leq 0.010$.

binding site was used, hypoxia or hypoxia-mimetic drugs induced repression of this reporter in a κB-dependent manner (Fig. 2B).

To investigate whether endogenous genes were being affected by hypoxia-induced NF-κB, mRNA analyses of IL-8 and PTEN were performed in several different cell lines (Fig. 2C and D). These experiments confirmed the luciferase reporter assays and demonstrated that hypoxic stress was inducing IL-8 mRNA while repressing PTEN mRNA. Furthermore, when we analyzed mouse endothelial cells, a primary cell line, we could verify that hypoxia was inducing two important chemokines, Cxcl1 and Cxcl2, both of which are functional homologues for human IL-8 (Fig. 2E).

To verify that NF-κB was responsible for these effects, we used selective siRNA oligonucleotides to inhibit NF-κB subunit activity (Fig. 3). Importantly, the inhibition of RelA prevented the repression of PTEN mRNA that was observed during hypoxia, indicating that RelA was indeed responsible for the inhibition of PTEN that we observed (Fig. 3). Knockdown of RelA also prevented hypoxia-induced IL-8 expression, while depletion of p100/p52 did not (Fig. 3).

Previous studies have suggested that IL-8 can also be a HIF-1α target (21). To investigate if this was the case, we specifically depleted HIF-1α using siRNA oligonucleotides in U2OS cells (Fig. 4A, center). HIF-1α inhibition prevented the induction of adrenomedulin (ADM), a known HIF-1α target, following hypoxia (Fig. 4A, right). Importantly, inhibition of HIF-1α had no effect on the level of hypoxia-induced IL-8

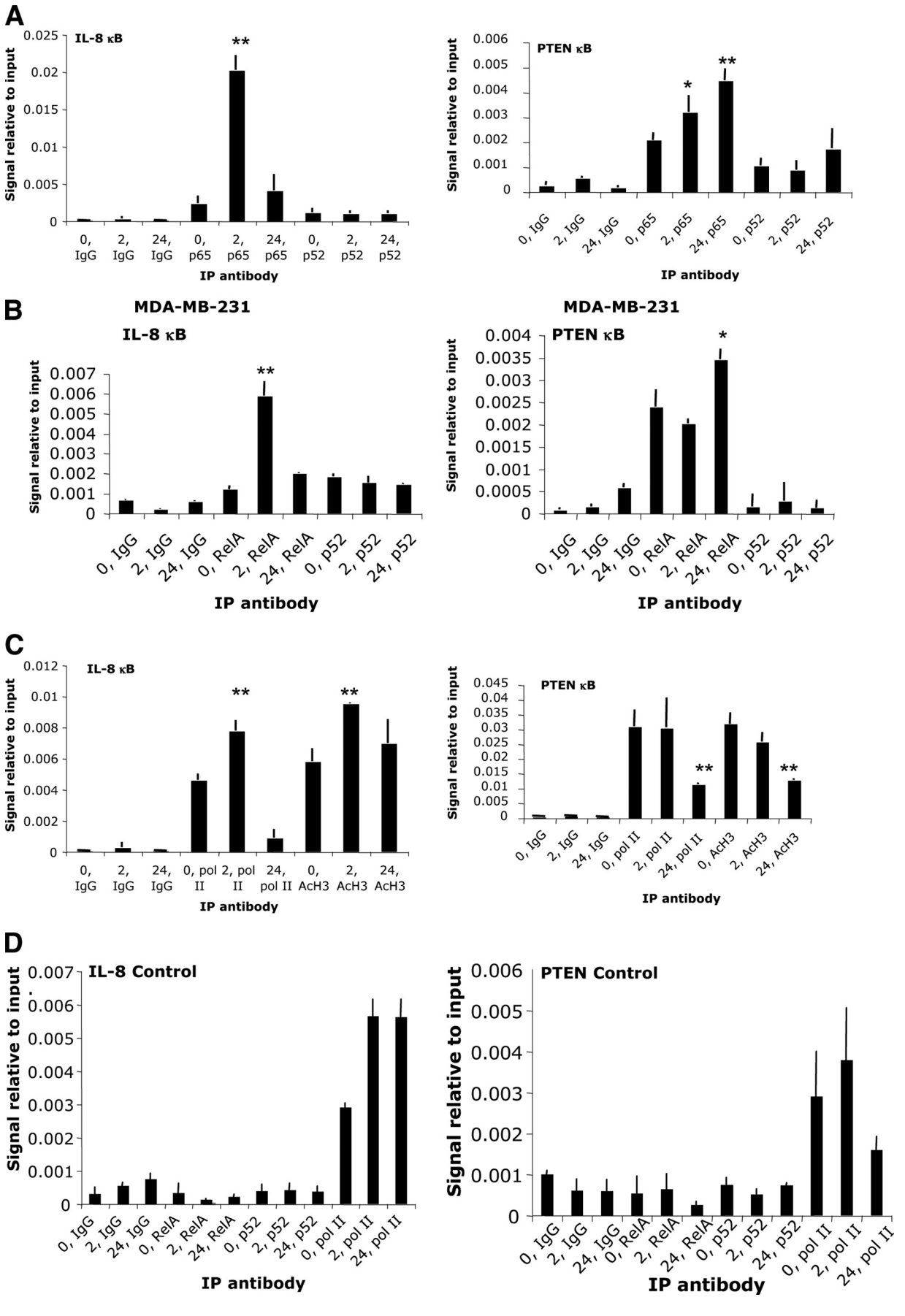
A
IL-8 κB
Signal relative to input
0.025
0.02
0.015
0.01
0.005
0
**
0, IgG
2, IgG
24, IgG
0, p65
2, p65
24, p65
0, p52
2, p52
24, p52
IP antibody
PTEN κB
0.006
0.005
0.004
0.003
0.002
0.001
0
*
**
0, IgG
2, IgG
24, IgG
0, p65
2, p65
24, p65
0, p52
2, p52
24, p52
IP antibody
B
MDA-MB-231
IL-8 κB
0.007
0.006
0.005
0.004
0.003
0.002
0.001
0
**
0, IgG
2, IgG
24, IgG
0, RelA
2, RelA
24, RelA
0, p52
2, p52
24, p52
IP antibody
MDA-MB-231
PTEN κB
0.004
0.0035
0.003
0.0025
0.002
0.0015
0.001
0.0005
0
*
0, IgG
2, IgG
24, IgG
0, RelA
2, RelA
24, RelA
0, p52
2, p52
24, p52
IP antibody
C
IL-8 κB
0.012
0.01
0.008
0.006
0.004
0.002
0
**
**
0, IgG
2, IgG
24, IgG
0, pol II
2, pol II
24, pol II
0, AcH3
2, AcH3
24, AcH3
IP antibody
PTEN κB
0.045
0.04
0.035
0.03
0.025
0.02
0.015
0.01
0.005
0
**
**
0, IgG
2, IgG
24, IgG
0, pol II
2, pol II
24, pol II
0, AcH3
2, AcH3
24, AcH3
IP antibody
D
IL-8 Control
0.007
0.006
0.005
0.004
0.003
0.002
0.001
0
0, IgG
2, IgG
24, IgG
0, RelA
2, RelA
24, RelA
0, p52
2, p52
24, p52
0, pol II
2, pol II
24, pol II
IP antibody
PTEN Control
0.006
0.005
0.004
0.003
0.002
0.001
0
0, IgG
2, IgG
24, IgG
0, RelA
2, RelA
24, RelA
0, p52
2, p52
24, p52
0, pol II
2, pol II
24, pol II
IP antibody

mRNA (Fig. 4A, left), indicating that NF-κB is the transcription factor responsible for IL-8 induction.

In addition to IL-8, we could also demonstrate that hypoxia induces the expression of the antiapoptotic gene IAP2 in a RelA-dependent manner (Fig. 4B to D). On the other hand, hypoxia does not induce p100 mRNA or protein expression (Fig. 4B and 3C). We also compared the response to hypoxia with the response to TNF-α treatment in U2OS cells (Fig. 4E). TNF-α induces the expression of IL-8, IAP2, and p100 mRNA; however, the peak of expression occurs at 4 h posttreatment (Fig. 4E). Interestingly, TNF-α treatment does not result in PTEN mRNA repression (Fig. 4E). These data suggest that the NF-κB-mediated responses to hypoxia and TNF-α differ.

Hypoxia induces RelA recruitment to the IL-8 and PTEN promoters. Our results demonstrate that RelA is required for hypoxia-induced IL-8 and PTEN repression (Fig. 2 to 4). To verify that IL-8 and PTEN are direct targets of NF-κB following hypoxia, we used chromatin immunoprecipitation analysis followed by qPCR to determine whether NF-κB was actively recruited to the promoters of these genes. Hypoxia induced RelA binding to both the IL-8 and the PTEN promoter with different kinetics (Fig. 5A and B). On the other hand, p52 was not recruited to these promoters (Fig. 5A and B), consistent with our siRNA analysis. Importantly, and mirroring our mRNA expression data, hypoxia induced transient increases in the levels of RNA polymerase II and acetylated H3 at the IL-8 promoter, while these hallmarks of active transcription were reduced in a time-dependent manner on the PTEN promoter (Fig. 5C). Significantly, when we analyzed the control regions of these genes, we could not detect any specific recruitment of NF-κB (Fig. 5D). These results confirm the direct and differential regulation of IL-8 and PTEN by NF-κB following hypoxic stress, and they demonstrate that hypoxia can modulate NF-κB in a promoter-dependent manner.

Hypoxia-induced NF-κB requires the IKK complex. We have found that hypoxia induces NF-κB DNA binding, RelA nuclear translocation, IKK and IκBα phosphorylation, and the modulation of specific NF-κB target genes (Fig. 1 to 5). Therefore, we focused our efforts on defining the mechanism of hypoxic induction of NF-κB. It has been suggested previously that hypoxia-induced tyrosine 42 (Tyr42) phosphorylation of IκBα is an IKK-independent modification. While we could detect a slight induction of IκBα Tyr42 phosphorylation by hypoxia, these levels were much lower than those for the controls treated with peroxide or pervanadate, which are known inducers of this modification, especially considering that there was much more protein in the hypoxia-treated samples (Fig. 6A). These results were also verified when we evaluated the levels of tyrosine phosphorylation of IκBα by using a very specific, validated antibody that recognizes tyrosine phosphorylation (Fig. 6B). Given these results, we hypothesized that hypoxia-induced NF-κB activation was IKK dependent.

To test this hypothesis, we used a chemical inhibitor of IKK in U2OS cells, as well as in IKKα/β-null mouse embryonic fibroblasts (MEFs). U2OS cells were pretreated with an IKK inhibitor for 30 min before hypoxia treatment, and the resulting lysates were analyzed for levels of IKK activity by Western blotting (Fig. 6C). IKK inhibition reduced TNF-α- and hypoxia-induced phosphorylation of IKK and IκBα. In addition, it reduced NF-κB DNA binding (Fig. 6D), suggesting that IKK activity is important for these effects. We confirmed these findings by comparing IKK wild-type MEFs to IKKα/β-null MEFs. Importantly, IKK deletion resulted in the prevention of NF-κB DNA binding (Fig. 6E). In addition, a complete lack of IκBα phosphorylation was evident in cells lacking IKKα/β or IKKγ/NEMO (Fig. 6F and G). Significant reductions in NF-κB DNA binding were also observed in MEFs with single deletions of IKKα and IKKβ, even following prolonged hypoxia exposure (Fig. 6H). Taken together, these data demonstrate, to our knowledge for the first time, that hypoxia-induced NF-κB DNA binding is IKK dependent.

Hypoxia-induced NF-κB requires TAK1, but TAB1 and TAB2 are not essential. Hypoxia induces the phosphorylation of IKK in its activation loop (Fig. 1 and 6). IKK activation is induced by upstream kinases within the mitogen-activated protein kinase (MAPK) family. Transforming growth factor β (TGF-β)-activated kinase 1 (TAK1; also called MAP3K7) is a member of this important family of kinases. TAK1 is crucial for IKK activation following treatment with TNF-α or other stimuli, such as IL-1β and LPS (34). Therefore, we hypothesized that TAK1 was also responsible for hypoxia-induced IKK and the subsequent NF-κB activity that we have observed. We used TAK1-null MEFs and compared them to matching wild-type control cells (Fig. 7A). We detected a severe impairment of NF-κB DNA binding in TAK1-deficient cells, while OCT-1 DNA binding was unaffected. Furthermore, when IKK activity was analyzed, a reduction in the level of phosphorylated IKK and almost-complete inhibition of IκBα Ser32/36 phosphorylation were seen (Fig. 7B). Taken together, these data suggest that TAK1 is critical to the hypoxia-induced activation of the NF-κB pathway via the IKK-IκBα axis.

We extended our analysis by using siRNA oligonucleotides specific for TAK1 (Fig. 7C and D). siRNA-mediated knockdown of TAK1 resulted in severe inhibition of the phosphorylation of both IKK and IκBα in U2OS and HeLa cells (Fig. 7C and D). In addition, the TAK1 chemical inhibitor 5Z-7-oxozeaenol also prevented hypoxia-induced IKK activity (Fig. 7E). Furthermore in the absence of TAK1, hypoxia did not induce the NF-κB-dependent expression of IAP2 (Fig. 7F). These data define, to our knowledge for the first time, the TAK1-

FIG. 5. Hypoxia induces the dynamic recruitment of RelA to the promoters of IL-8 and PTEN with opposing transcriptional outcomes. (A and B) U2OS (A) and MDA-MB-231 (B) cells were exposed to 1% O_2 for the indicated periods prior to being cross-linked and harvested for ChIP analysis. Following immunoprecipitation (IP) with the indicated antibodies, DNA was purified and analyzed by qPCR using primers specific for the indicated promoters. (C) U2OS cells were treated as for panel A, and RNA polymerase II (Pol II) occupancy and the levels of acetylated H3 (AcH3) at the IL-8 and PTEN promoters were analyzed by qPCR. (D) U2OS cells were treated as for panel A, and the levels of RelA and p52 at the control regions of the IL-8 and PTEN genes were analyzed by qPCR. *, $P \leq 0.050$; **, $P \leq 0.010$.

dependent activation of NF-κB via the IKK complex in response to hypoxia.

In cells, TAK1 is present in a complex with TAB1 and TAB2/3 (1). We therefore investigated whether TAB1 or TAB2 was required for TAK1 function in the context of hypoxia-induced NF-κB. For this purpose, we used TAB1- and TAB2-null MEFs and corresponding wild-type MEFs (Fig. 7G and H). Our results show that even in the absence of TAB1 or TAB2, hypoxia is still able to induce the IKK–NF-κB pathway. TAB1 (Fig. 7G)- and TAB2 (Fig. 7H)-null cells still possessed hallmarks of IKK activation. To firmly establish that TAK is capable of activating IKK, we overexpressed a TAK1–TAB1 fusion protein that makes TAK1 constitutively active (Fig. 7I). We could observe that overexpression of the fusion protein was sufficient to induce the activation of IKK (Fig. 7I). These data indicate that TAK1 is essential for hypoxia-induced IKK-NF-κB.

Hypoxia-induced IKK and IκBα phosphorylation is PHD1, PHD2, PHD3, and HIF-1α independent. The response to hypoxia is mediated by critical oxygen-sensing enzymes (17). The PHD enzymes require oxygen in addition to iron and 2-oxoglutarate for full activity; therefore, the reduction in oxygen levels results in the inhibition of PHD function and the stabilization of HIF-α subunits. Therefore, we wanted to determine if either the loss of function of the PHD enzymes as a result of low oxygen tension or the resulting stabilization of HIF-1α itself was involved in the complex activation of NF-κB in response to hypoxia. We transiently depleted PHD1, PHD2, and PHD3, and we also generated stable knockdown cells by using shRNA technology. It would be predicted that if any of these enzymes were involved in the process of hypoxia-induced NF-κB, their depletion should result in higher levels of IKK activation in normoxia. We found that phosphorylation of both IKK and IκBα was largely unaffected by knockdown of the PHD enzymes (Fig. 8A to D). These data show that the loss of PHD function that occurs under hypoxic conditions does not contribute significantly to the increases in IKK or IκBα phosphorylation.

To determine if hypoxia-induced IKK–NF-κB was a result of HIF-1α activity or stabilization, we analyzed the levels of phosphorylation of IKK and IκBα in stable HIF-1α-depleted cells and compared these to the levels in control cells (Fig. 8E and F). Our data clearly demonstrate that even in the absence of HIF-1α, both IKK and IκBα are readily phosphorylated in response to hypoxia (Fig. 8F); therefore, this is a HIF-1α-independent process.

Hypoxia-induced NF-κB activation requires Ca^{2+} and CaM kinase 2 and Ubc13. Several upstream factors, including receptor adaptor molecules and calcium calmodulin kinases, have been reported to be important for TAK1 and IKK activation in response to various stimuli. Given our finding that TAK1 is required for hypoxia-induced NF-κB activity (Fig. 8), the involvement of these upstream factors was investigated (Fig. 9 to 11). TAK1-mediated activation of the IKK complex in response to both TNF-α and IL-1β has been reported previously (34). In both cases, binding of the ligand to the specific membrane receptor is required for the activation of the TAK1-dependent cellular signaling cascade leading to NF-κB activation (35). We wanted to determine if TRAF2 or TRAF6, two adaptor proteins important for TNF-α and IL-1β signaling, respectively, was necessary for hypoxia-induced NF-κB.

We used lysates obtained from TRAF2-null, TRAF6-null, and wild-type control MEFs treated with 1% O_2 for varying lengths of time. TRAF2 and TRAF6 were dispensable for hypoxia-induced IKK–NF-κB (Fig. 9A and B). Similar levels of NF-κB DNA binding following hypoxia were observed for wild-type and null cells (data not shown). Interestingly, TRAF6-null cells possess a very low level of IκBα protein, as detected by Western blotting, making the determination of phosphorylated-IκBα levels very difficult (Fig. 9B). However, IKK phosphorylation levels were readily detected and revealed no differences between genotypes (Fig. 9B).

The cellular response to hypoxic stress has also been shown to induce a DNA damage checkpoint response and endoplasmic reticulum (ER) stress. We did not find any role for these pathways in the process of NF-κB activation following hypoxia (Fig. 9C to E).

Hypoxia has previously been reported to induce the activity of calcium/calmodulin-dependent kinase 2 (CaMK2) (5). Moreover, CaMK2 was recently shown to interact directly with and activate TAK1 in response to TLR signaling (25). To determine if there is a role for this enzyme in the TAK1-dependent activation of NF-κB in the context of hypoxia, we used the CaMK2 inhibitor KN-93 (Fig. 10A). While this inhibitor was not completely effective, it reduced the levels of IKK and IκBα phosphorylation induced by hypoxia (Fig. 10A). However, when we used a specific siRNA targeting CaMK2δ, a major subunit expressed in osteosarcoma cells (Fig. 10B), there was a visible reduction in both IKK and IκBα phosphorylation (Fig. 10C). Furthermore, depletion of CaMK2δ prevented the induction of IL-8 mRNA by hypoxia (Fig. 10D). These results suggest that Ca^{2+} release is the signal for TAK1–IKK–NF-κB activation following hypoxia. To test this hypothesis, we induced Ca^{2+} release by treatment with the Ca^{2+} pump inhibitor thapsigargin for 1 h. After this period, we exposed cells to hypoxia and analyzed the IKK activation pattern (Fig. 10E). Cells that had been pretreated with this compound, and therefore had decreased Ca^{2+} stores, exhibited severely impaired levels of IKK and IκBα phosphorylation (Fig. 10E). In addition, we investigated whether increased CaMK2 expression was sufficient to activate IKK (Fig. 10F). For this purpose, we overexpressed CaMK2δ and analyzed the hallmarks of IKK activation. We could observe increased levels of both IKK and IκBα phosphorylation in response to CAMK2δ overexpression (Fig. 10F). Taken together, these data demonstrate that while TRAF2, TRAF6, ATM, and PERK are not required for TAK1-dependent hypoxia-induced NF-κB activation, Ca^{2+} release and CaMK2 are necessary for both IKK and IκBα phosphorylation in response to hypoxia.

In addition to adaptor molecules, activation of NF-κB is dependent on an intricate network of ubiquitin-conjugating complexes (39). As such, complexes containing Ubc13 and UbcH5 have been shown to be required for NF-κB activation both *in vitro* and *in vivo* (1). Very recently, a novel form of ubiquitin chain was shown to be critical for activation of the IKK complex in response to a variety of known NF-κB-activating stimuli (41). The complex identified, LUBAC (linear ubiquitin chain assembly complex), promotes the conjugation of linear chains onto Nemo, which is required for full activa-

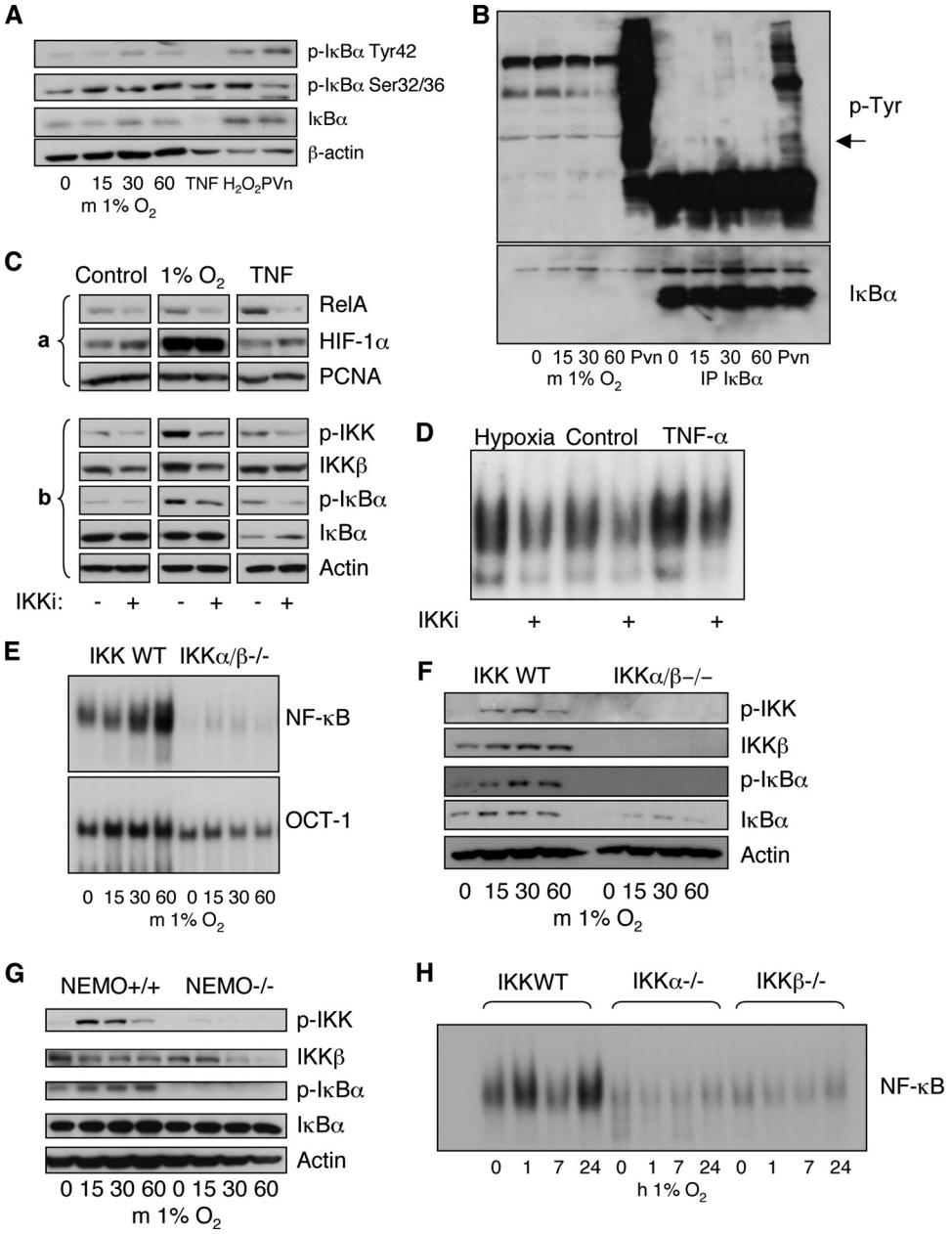

FIG. 6. Hypoxia-induced NF-κB requires the IKK complex. (A) U2OS cells either were treated with 1% O_2 for the indicated times or were treated with 10 ng/ml TNF-α, 50 μM H_2O_2, or 100 μM pervanadate (PVn) for 30 min prior to harvest, and cytoplasmic/nuclear extracts were prepared. Protein extracts were analyzed by Western blotting. (B) U2OS cells either were treated with 1% O_2 for the indicated times or were treated with 100 μM pervanadate for 30 min prior to harvest. Two hundred micrograms of the total-cell lysate was used to immunoprecipitate IκBα. Immunoprecipitated material was analyzed by Western blotting. (C) U2OS cells were pretreated with the IKK inhibitor (IKKi) 20 μM Bay 117082 30 min prior to treatment with 1% O_2 or 10 ng/ml TNF-α for an additional 30 min. Cells were then harvested, and nuclear (a) and cytoplasmic (b) extracts were obtained. These were analyzed by Western blotting. (D) Nuclear extracts obtained in the experiment described for panel C were analyzed by EMSA. (E) Wild-type IKK and IKKα/β-null MEFs were treated with 1% O_2 for the indicated times prior to harvest, and nuclear and cytoplasmic extracts were obtained. Nuclear extracts were analyzed by EMSA for NF-κB and OCT-1 DNA binding. (F) Cytoplasmic extracts obtained as described for panel E were analyzed by Western blotting. (G) Wild-type and Nemo/IKKγ-null MEFs were exposed to 1% O_2 for the indicated periods prior to lysis, and cytoplasmic/nuclear extracts were prepared. Cytoplasmic extracts were analyzed by Western blotting. (H) MEFs with wild-type IKK (IKKWT) and IKKα- and IKKβ-null MEFS were treated with 1% O_2 for the indicated times, and nuclear extracts were obtained. NF-κB DNA binding activity was analyzed by EMSA.

tion of the IKK complex (41). Given the unusual nature of the hypoxia-activated pathway leading to NF-κB activation, we next determined if any of the ubiquitin-conjugating complexes is required for the induction of NF-κB by hypoxia. siRNA oligonucleotides directed toward Ubc13, UbcH5a, HOIP, and HOIL-1L (LUBAC) were used in combination with hypoxia exposure (Fig. 11). Our analysis revealed that only depletion of Ubc13 prevented both IKK and IκBα phosphorylation follow-

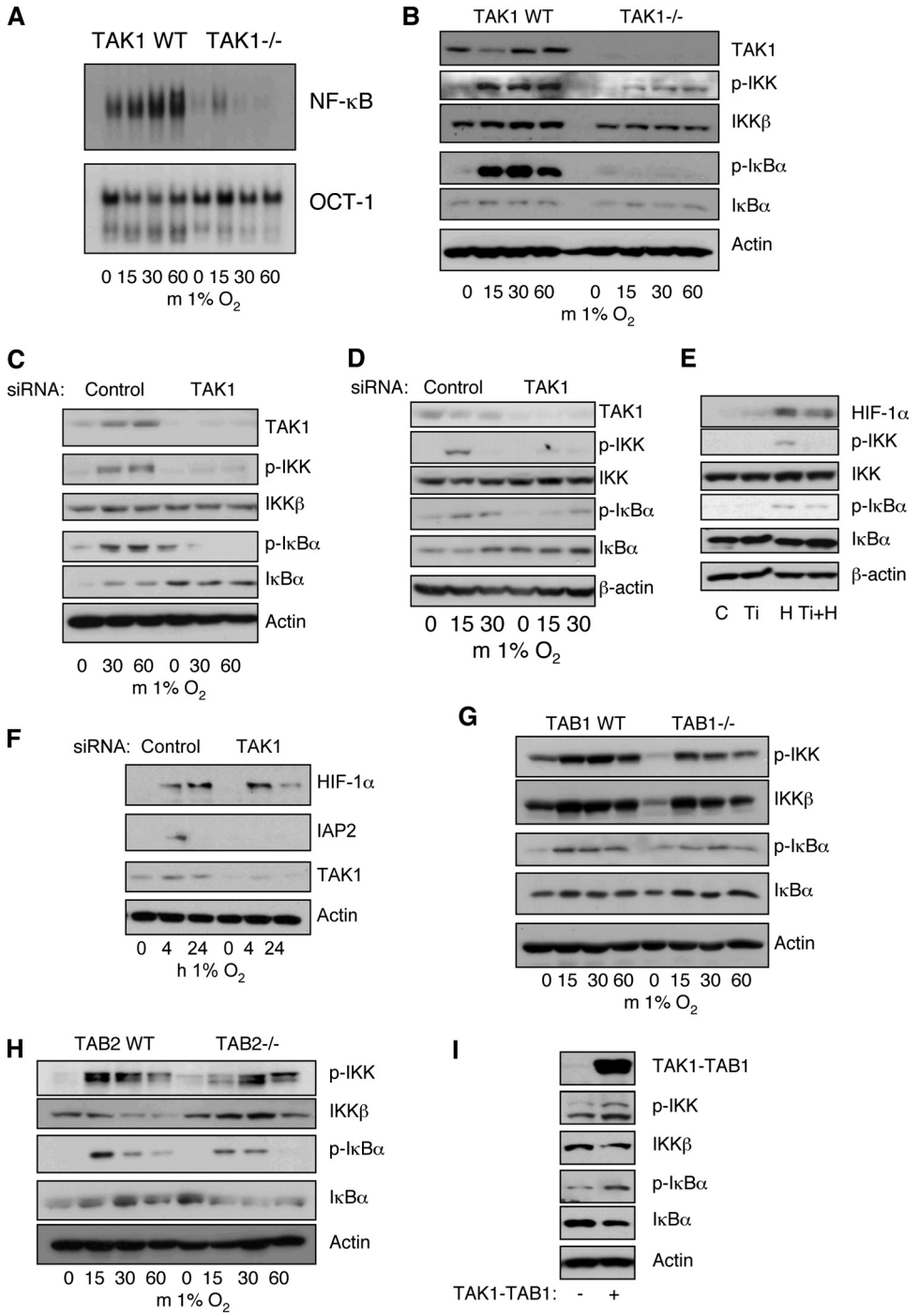

FIG. 7. Hypoxia-induced IKK-NF-κB is TAK1 dependent. (A) MEFs with wild-type (WT) TAK1 and TAK1-null MEFS were exposed to 1% O_2 for the indicated periods prior to being harvested, and cytoplasmic/nuclear extracts were obtained. Nuclear extracts were analyzed by EMSA for the DNA binding activities of NF-κB and OCT-1. (B) Cytoplasmic extracts obtained as for panel A were analyzed by Western blotting. (C and D) U2OS (C) and HeLa (D) cells were transfected with the indicated siRNA oligonucleotides 48 h prior to harvest. Thirty minutes and 15 min prior to lysis, cells were exposed to 1% O_2. Whole-cell lysates were analyzed by Western blotting. (E) TAK1 inhibition reduces hypoxia-induced IKK activity. U2OS cells were pretreated with 1 μM 5Z-7-oxozeaenol for 45 min prior to treatment with 1% O_2 for an additional 30 min. Nuclear and cytoplasmic extracts were prepared and were analyzed by Western blotting. C, control; Ti, TAK inhibitor; H, hypoxia. (F) U2OS cells were transfected with control and TAK1 siRNA oligonucleotides prior to being exposed to 1% O_2 for the indicated times. Whole-cell lysates were analyzed by Western blotting. (G) MEFs with wild-type TAB1 and TAB1-null MEFs were exposed to 1% O_2 for the indicated times prior to being harvested. Cytoplasmic extracts were analyzed by Western blotting. (H) MEFs with wild-type TAB2 and TAB2-null MEFs were exposed to 1% O_2 for the indicated times prior to being harvested. Cytoplasmic extracts were analyzed by Western blotting. (I) U2OS cells were transfected with 1 μg of a control construct or a GST-TAK-TAB1 fusion construct for 48 h prior to harvest. Whole-cell lysates were analyzed by Western blotting.

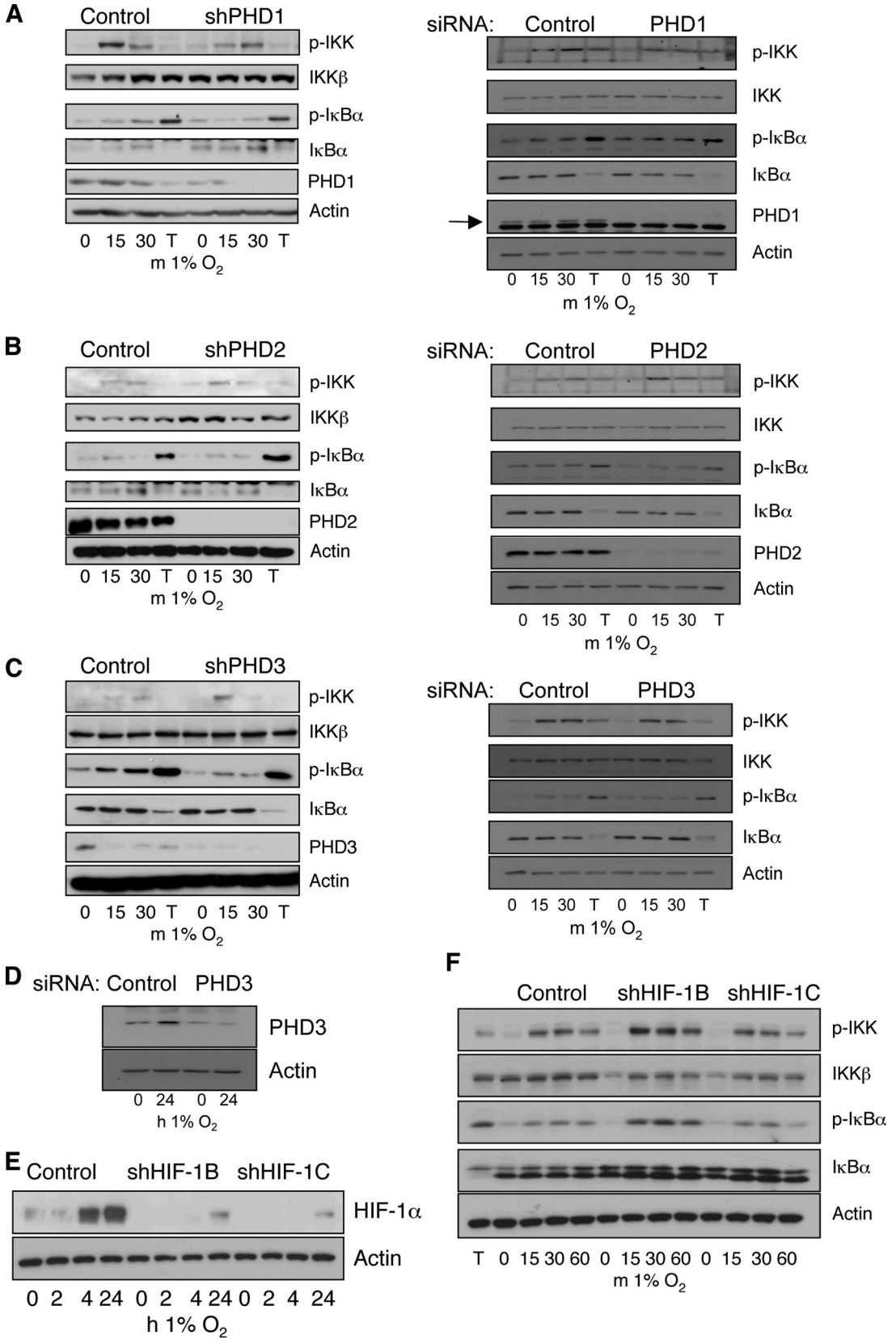

FIG. 8. Hypoxia-induced IKK is PHD1, PHD2, PHD3, and HIF-1α independent. U2OS cells were transiently (right) or stably (left) depleted of PHD1 (A) (arrow indicates specific band), PHD2 (B), or PHD3 (C and D) or were stably depleted of HIF-1α (E and F). Cells were exposed to 1% O_2 for the indicated times or to 10 ng/ml TNF-α (T) for 30 min prior to lysis. Whole-cell lysates were analyzed by Western blotting.

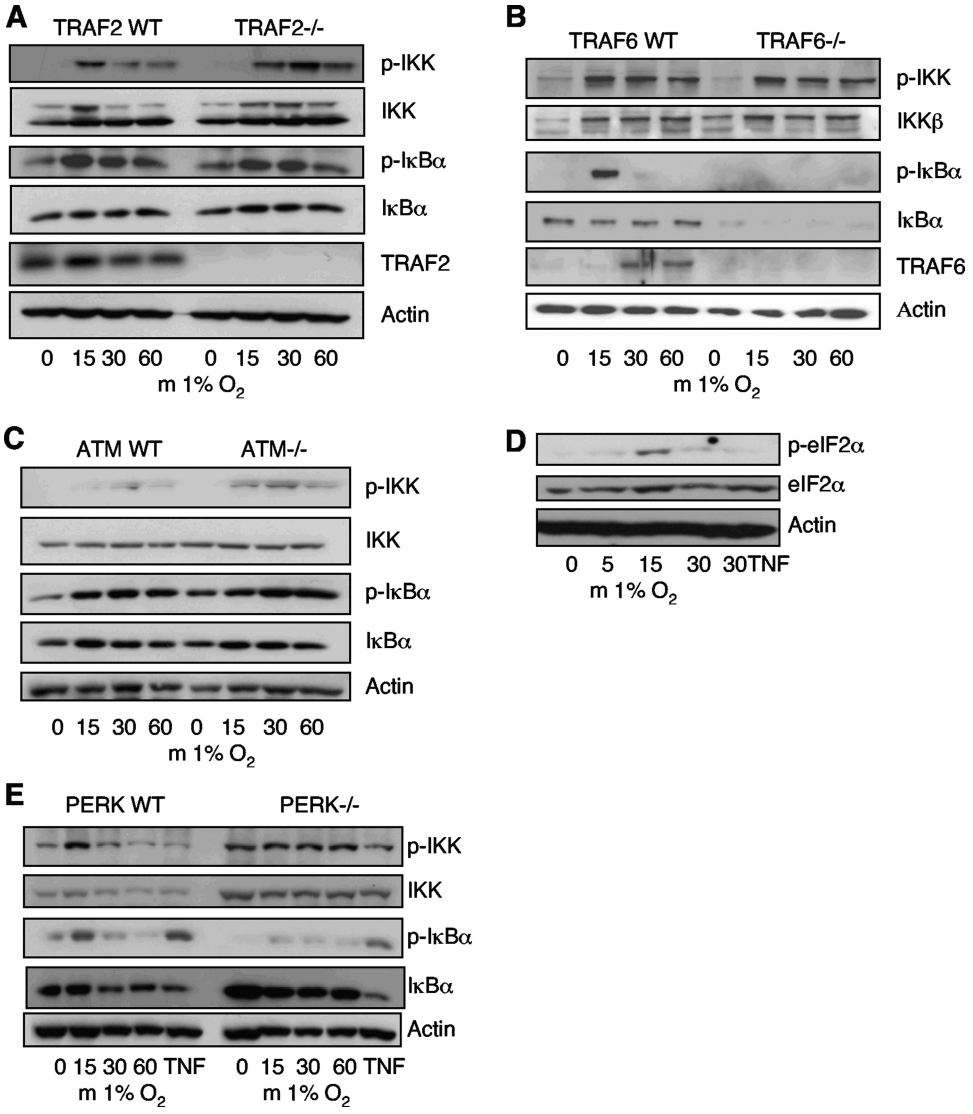

FIG. 9. Hypoxia-induced TAK1-IKK-NF-κB does not involve TRAF2, TRAF6, PERK, or ATM. (A) MEFs with wild-type (WT) TRAF2 and TRAF2-null MEFs were exposed to 1% O_2 for the indicated periods prior to being harvested. Cytoplasmic extracts were analyzed by Western blotting. (B) MEFs with wild-type TRAF6 and TRAF6-null MEFs were treated and analyzed as for panel A. (C) ATM-null and reconstituted ATM cells were treated and analyzed as for panel A. (D) U2OS cells were exposed to 1% O_2 for the indicated times or to 30 min of 10 ng/ml TNF-α prior to lysis, and whole-cell lysates were analyzed by Western blotting. (E) MEFs with wild-type PERK and PERK-null MEFS were treated and analyzed as for panel A. These cells were also treated with 10 ng/ml TNF-α for 30 min prior to being analyzed.

ing hypoxic stress (Fig. 11A). Depletion of the LUBAC components HOIP and HOIL-1L or of UbcH5a did not affect IKK activity (Fig. 11B and C). These findings elucidate a novel pathway of NF-κB activation in response to hypoxia characterized not only by calcium release and CAMK2 activity but also by Ubc13.

Hypoxia induces IκBα sumoylation by Sumo-2/3. Since hypoxia-induced NF-κB is dependent on the IKK complex but does not result in IκBα degradation, we wanted to determine the ubiquitin and ubiquitin-like modification status of IκBα in response to hypoxia. Following TNF-α treatment, IκBα undergoes lysine 48-linked ubiquitination, which results in the rapid targeting of IκBα for proteasomal degradation. We used the proteasome inhibitor MG132, to allow the accumulation of modified IκBα, and compared 1% O_2 treatment to TNF-α treatment. While TNF-α treatment resulted in the accumulation of slower-migrating forms of IκBα, consistent with ubiquitination (Fig. 12A, lanes 5 and 6), hypoxia treatment did not result in any significant increase in these forms of IκBα (Fig. 12A, lanes 3 and 4). These data suggest that in hypoxia, IκBα either fails to be ubiquitinated or is very rapidly deubiquitinated. In order to distinguish between these possibilities, we assessed whether TNF-α still promoted IκBα degradation in the presence of hypoxia (Fig. 12B). When cells were exposed to 1% O_2 for 5 min and were then treated with 10 ng/ml TNF-α, IκBα was no longer degraded (Fig. 12B). This result suggested that hypoxia prevents IκBα ubiquitination.

Since hypoxia prevented TNF-α-induced IκBα degradation,

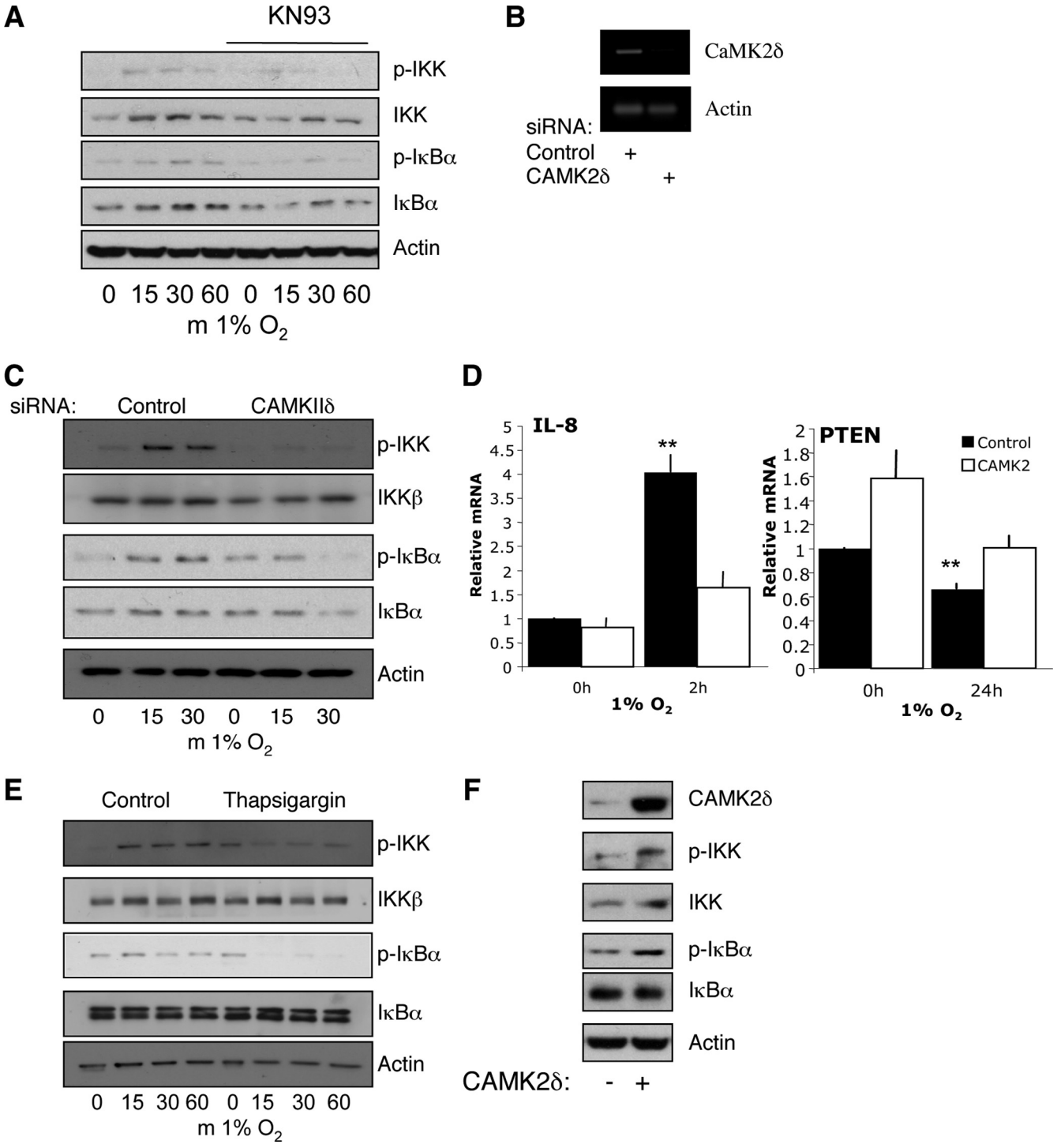

FIG. 10. Hypoxia-induced TAK1-IKK-NF-κB requires Ca^{2+} and CAMK2. (A) U2OS cells were treated with 2 μM KN-93 30 min prior to exposure to 1% O_2 for the indicated times. Whole-cell lysates were analyzed by Western blotting. (B) U2OS cells were transfected with a control or a CaMK2δ siRNA oligonucleotide, and the level of knockdown was assessed by RT-PCR. (C) U2OS cells were transfected as for panel B and were exposed to 1% O_2 for the indicate times prior to lysis. Whole-cell lysates were analyzed by Western blotting. (D) U2OS cells were transfected as for panel B prior to exposure to 1% O_2 for the indicated times and RNA extraction. IL-8 and PTEN mRNAs were analyzed by qPCR. *, $P \leq 0.050$; **, $P \leq 0.010$. (E) U2OS cells were treated with 1 μM thapsigargin for 1 h prior to exposure to 1% O_2 for the indicated periods. Whole-cell lysates were analyzed by Western blotting. (F) U2OS cells were transfected with 1 μg of a control or a CAMK2δ construct for 48 h prior to harvest. Whole-cell lysates were analyzed by Western blotting.

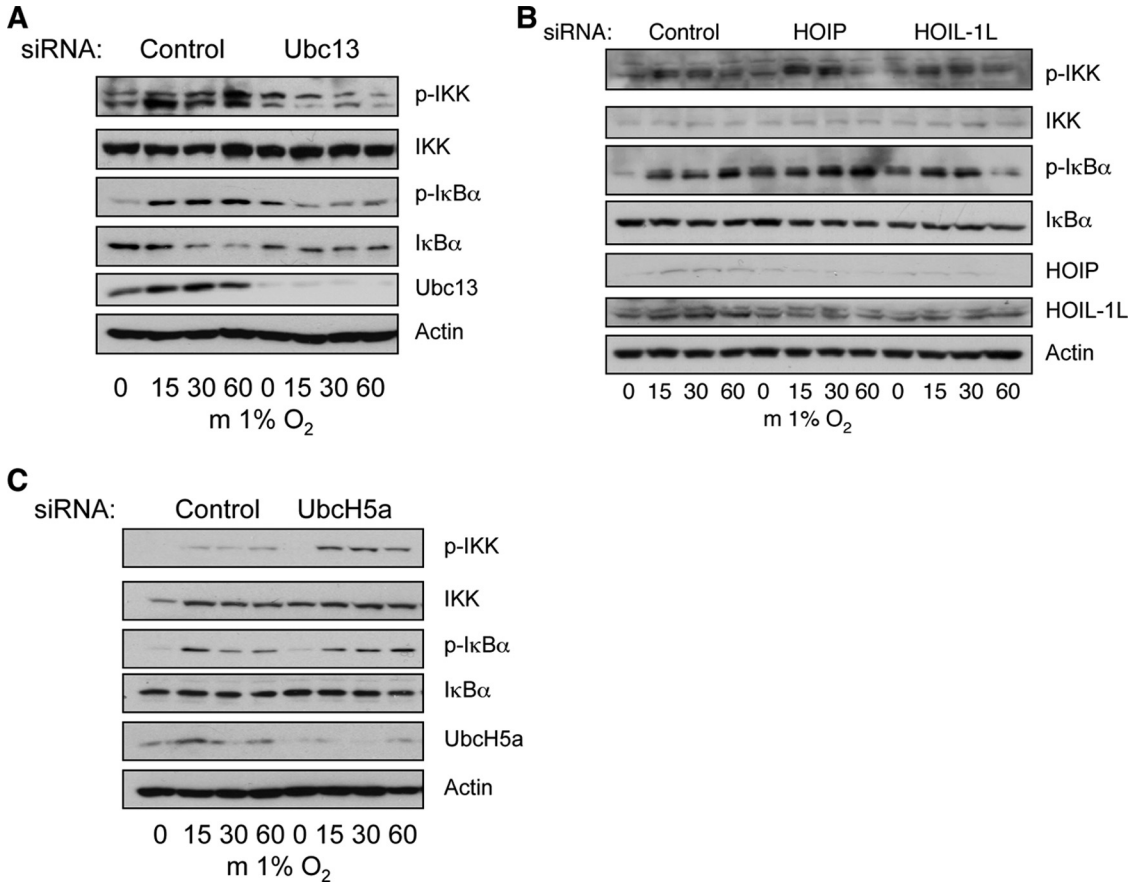

FIG. 11. Hypoxia-induced TAK1-IKK-NF-κB requires Ubc13 but not UbcH5 or LUBAC. (A) U2OS cells were transfected with the indicated siRNA oligonucleotides and were exposed to 1% O_2 for the indicated times before lysis. Whole-cell lysates were analyzed by Western blotting. (B) U2OS cells were transfected with a control, HOIP, or HOIL-1L siRNA oligonucleotide prior to being treated and processed as for panel A. (C) U2OS cells were transfected with a control or a UbcH5a siRNA oligonucleotide prior being treated and processed as for panel A.

we hypothesized that other modifications might be occurring on IκBα in response to hypoxia that could account for this novel regulation and activation of NF-κB. For this purpose, we used His-tagged versions of ubiquitin and ubiquitin-like modifiers, with or without hypoxia treatment, and performed Ni^{2+} purification under denaturing conditions. Ni^{2+} pulldown eluates were then analyzed for their IκBα profiles. We validated this system using TNF-α treatment and demonstrated that, as expected, IκBα was inducibly ubiquitinated (Fig. 12C). Our experiments revealed that while IκBα modification with ubiquitin and Nedd8 does not occur following hypoxia treatment (Fig. 12D), conjugation with Sumo-2/3 is increased (Fig. 12E).

Furthermore, Sumo-2/3 conjugation occurs on lysine 21 of IκBα, since mutation of this site prevents Sumo-2 conjugation (Fig. 12F). We also analyzed the Sumo-2/3 conjugation pattern of IκBα mutated at tyrosine 42. Although this mutation resulted in a different mobility pattern for IκBα on the gel, Sumo-2/3 conjugation occurred to a higher level than for wild-type IκBα, and hypoxia did not significantly change this (Fig. 12F). These data demonstrate that hypoxia induces differential posttranslational modification of IκBα, and they suggest that sumoylation prevents IκBα degradation during hypoxia. To test this possibility, we performed siRNA-mediated knockdown of the known Sumo proteases (Senps) and either left these cells untreated or treated them with TNF-α. While control and Senp1-depleted cells were still able to degrade IκBα in response to TNF-α, depletion of Senp2, Senp3, Senp5, Senp6, or Senp7 prevented IκBα degradation (Fig. 13A and B). Similarly, when Senp1 and Senp2 were co-overexpressed, hypoxia induced IκBα degradation (Fig. 13C). Since hypoxia induces NF-κB activity and we identified Sumo-2/3 conjugation to IκBα, we tested whether prevention of desumoylation by these Senps affected NF-κB–IκBα interaction. We performed siRNA-mediated knockdown of the Senps and analyzed the amount of RelA bound to IκBα by coimmunoprecipitation (Fig. 13D). Depletion of Senp3, Senp5, Senp6, or Senp7 resulted in a decreased association between RelA and IκBα, with Senp6 and Senp7 producing higher degrees of IκBα dissociation. These results indicate that modulation of the Sumo conjugation status of IκBα has a direct impact on NF-κB release.

To verify that RelA released from IκBα was active, we analyzed the transcript levels of two NF-κB targets, IL-8 and IAP2 (Fig. 13E). Depletion of Senp5, Senp6, or Senp7 induced upregulation of IL-8 and IAP2 mRNAs (Fig. 13E) and IAP2 protein (Fig. 13F). Taken together, these data demonstrate the novel and differential posttranslational regulation of IκBα, as part of the regulation of NF-κB activity during hypoxia.

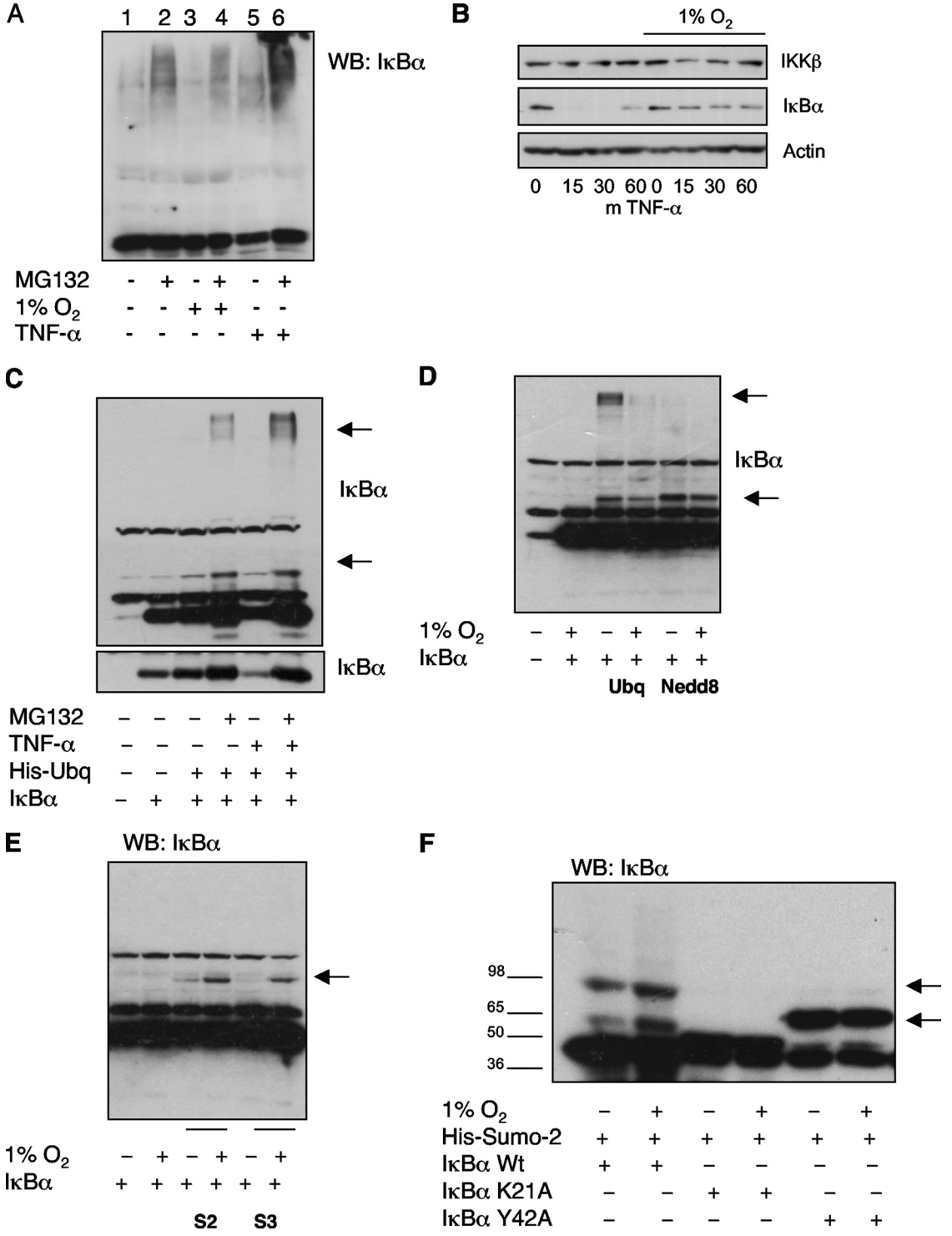

FIG. 12. Hypoxia-promoted Sumo-2/3 conjugation to IκBα prevents its degradation. (A) U2OS cells were treated with the proteasome inhibitor MG132 3 h prior to a 30-min treatment with 1% O_2 or 10 ng/ml TNF-α. Cells were harvested directly into SDS loading buffer, and IκBα levels were determined by Western blotting (WB). (B) U2OS cells were treated with TNF-α for the indicated periods in the presence or absence of 1% O_2 prior to lysis. Whole-cell lysates were analyzed by Western blotting. (C) HEK293 cells were transfected with 1 μg of IκBα and 1 μg of His_6-ubiquitin, and where indicated, they were treated with TNF-α or MG132, or both. Ubiquitinated proteins were purified using Ni^{2+} agarose, and pulldown eluates were analyzed by Western blotting for IκBα. Arrows indicate modified versions of IκBα. (D) HEK293 cells were transfected with 1 μg of IκBα and 1 μg of a His-tagged version of ubiquitin or Nedd8 where indicated. Cells were treated or not with 1% O_2 for 15 min and were harvested 48 h posttransfection. Extracts were processed and analyzed as for panel C. Arrows indicate modified versions of IκBα. (E) HEK293 cells were transfected with 1 μg of IκBα and 1 μg of a His-tagged version of Sumo-2 (S2) or Sumo-3 (S3) where indicated. Cells were treated or not with 1% O_2 for 15 min and were harvested 48 h posttransfection. Extracts were processed and analyzed as for panel C. Arrows indicate modified versions of IκBα. (F) Sumo-2 is conjugated to lysine 21 of IκBα. HEK293 cells were treated with1 μg of wild-type (Wt) or K21A or Y42A mutant IκBα and were exposed or not to 1% O_2 for 15 min prior to lysis. Sumoylated proteins were purified as for panel C, and pulldown eluates were analyzed for IκBα by Western blotting. Arrows indicate modified versions of IκBα.

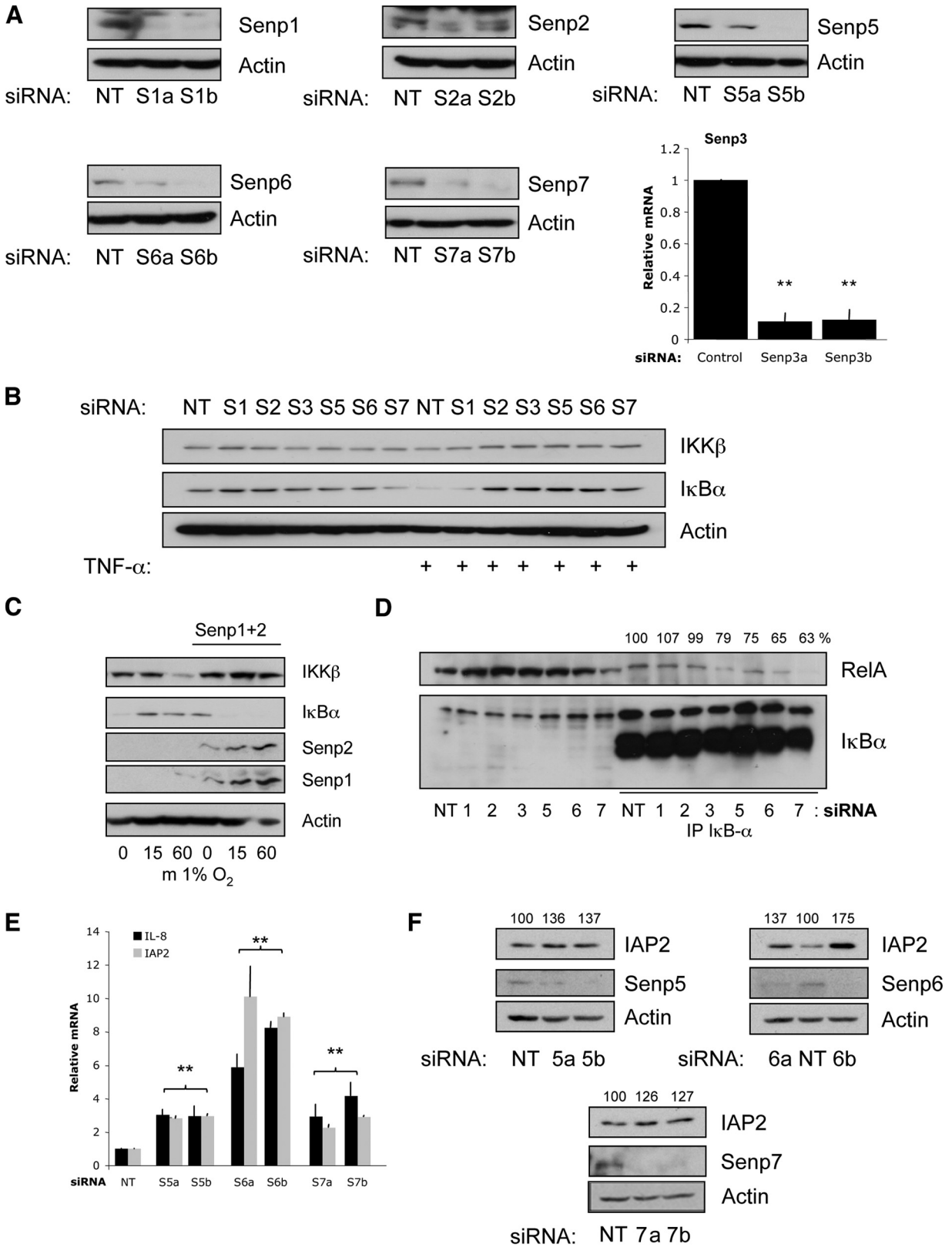

FIG. 13. Hypoxia-promoted Sumo-2/3 conjugation to IκBα prevents its degradation but results in NF-κB activation. (A) U2OS cells were transfected with the indicated siRNA oligonucleotides prior to lysis. Whole-cell lysates were analyzed by Western blotting. Senp3 levels were analyzed by qPCR. *, $P \leq 0.050$; **, $P \leq 0.010$. NT, nontargeted. (B) U2OS cells were transfected with the indicated siRNA oligonucleotides and were either left untreated or treated with 10 ng/ml TNF-α for 30 min prior to lysis. Whole-cell lysates were analyzed by Western blotting. (C) U2OS cells were transfected with either 2 μg of an empty control vector or 1 μg of Senp1 and 1 μg of Senp2. Cells were either left untreated or treated

DISCUSSION

Here we have investigated the mechanism of activation of the NF-κB family of transcription factors following hypoxic stress. Although hypoxia-induced NF-κB DNA binding was first described more than a decade ago (22), the mechanism behind it has not yet been defined. We have found that NF-κB activation following hypoxia is very rapid and persistent (Fig. 1 to 6). In addition, hypoxia induces NF-κB in an IKK (Fig. 6)- and TAK1 (Fig. 7)-dependent manner. However, this induction does not require either the molecular oxygen sensors PHD1 to PHD3, HIF-1α (Fig. 8), or the adaptor molecules TRAF2 and TRAF6 (Fig. 9). We find that TAK1 and IKK are activated by a mechanism involving Ca^{2+} release and CaMK2 (Fig. 10). Interestingly, we have uncovered a mechanism by which sumoylation of IκBα by Sumo-2/3, despite preventing IκBα degradation, results in NF-κB activation (Fig. 12 to 13).

Induction of IKK–NF-κB by hypoxia occurs very rapidly in a variety of different cell lines, ranging from 5 to 30 min (Fig. 1 to 4). In such a short time, no transcriptional responses are possible. Since oxygen is able to diffuse in and out of the cell, there should be an alternative mechanism of IKK activation. One of the rapid responses that hypoxia elicits is Ca^{2+} release from intracellular compartments, such as the ER (40). Although the exact mechanism of Ca^{2+} release differs from cell to cell, a recent study identified two parallel pathways that act, in hypoxia, to increase intracellular Ca^{2+} levels (2). Many of the cellular responses to Ca^{2+} release are mediated by a family of serine/threonine kinases called calcium/calmodulin-dependent kinases (CaMKs). CaMKs are responsible for a number of functions, such as mitochondria biogenesis and muscle plasticity (7). Importantly, the CaMK connection with NF-κB in response to Toll-like receptor (TLR)-mediated signaling was recently described in a study where CaMK2 was shown to directly bind and activate TAK1 (25). Similarly, we have found that CAMK2 inhibition, by several methods, prevents hypoxia-induced IKK phosphorylation and activity (Fig. 10). To our knowledge, this is the first mechanism described for the initial activation of NF-κB following hypoxic stress.

Hypoxia also induces NF-κB DNA target gene modulation (Fig. 2 to 5). Using specific target gene promoters fused to luciferase, we found that hypoxia can modulate NF-κB transcription activity in a promoter-dependent manner (Fig. 2A). However, when we used an artificial luciferase reporter construct, we observed that hypoxia induced a repression of NF-κB activity (Fig. 2B). This was also true for the hypoxia-mimetic drug desferrioxamine (DFX) and HIF-1α overexpression. These results suggest that artificial promoters can lead to artifactual results, due perhaps to the lack of the correct chromatin environment. Given this discrepancy, we validated the modulation of endogenous NF-κB target genes by analyzing endogenous mRNA levels and by performing ChIP analysis. Our results demonstrate that hypoxia induces IL-8 and IAP2 but represses PTEN in a RelA-dependent manner (Fig. 2 to 4). We find that RelA is actively recruited to the IL-8 and PTEN gene promoters (Fig. 5A and B), with opposing consequences for the levels of acetylated H3 and RNA polymerase II recruitment (Fig. 5C). It is likely that many other NF-κB targets are differentially modulated following hypoxia, and future studies will help define them. The reason why certain targets are activated at a particular time is a matter of much interest in the NF-κB research field. A combination of several factors can play a role in the decision-making process. As such, multiple posttranslational modifications have been described for some of the NF-κB subunits, which might explain modulation of activity (30). The availability of a coactivator and a corepressor might also explain the specificity of a NF-κB response. A more in-depth analysis of NF-κB might be useful in determining how hypoxia modulates the NF-κB response in the nucleus. The physiological relevance of our findings is underpinned by published studies of humans, where IL-8 was shown to increase very rapidly in people exposed to reduced oxygen tensions (12, 23, 28). Furthermore, the reduction in the level of PTEN (a negative regulator of the phosphatidylinositol 3-kinase pathway) and the increase in the level of IAP2 (an antiapoptotic protein) are consistent with a survival response to hypoxia.

We find that hypoxia-induced NF-κB is IKK and TAK1 dependent (Fig. 6 and 7). The IKK dependence is in accordance with a recent study where NF-κB activation following prolonged hypoxia exposure was studied (3). In that study, prolonged NF-κB activation following hypoxia was regulated by the activity of Cyld. Cyld is a negative regulator of IKK activation through its deubiquitinase activity (8). An and colleagues found that in cells expressing the E6 viral protein, prolonged hypoxia reduced the levels of Cyld, resulting in higher levels of IKK activity (3). We have deliberately used cell lines that do not possess E6 viral protein. These include transformed (U2OS, MDA-MB-231) and nontransformed (MCF10A, MEFs) cell lines, as well as primary cells (MEC). In all of these cells, we find that NF-κB is activated by hypoxia, leading to target gene modulation. It is noteworthy that in the study by An et al., Cyld levels did not change in the first hour of hypoxia exposure, indicating that Cyld inhibition is a secondary/parallel mechanism for NF-κB activation. Moreover, we have identified the requirement of Ubc13 for hypoxia-induced TAK1–IKK activity (Fig. 11A). Ubc13 mediates the conjugation of K63-linked ubiquitin to Nemo, which is normally counteracted by Cyld (8). In addition, Ubc13 levels were upregulated by hypoxia (Fig. 11A; also data not shown). It is possible that other pathways, both dependent and independent

with 1% O_2 for the indicated times and were harvested 48 h posttransfection. Whole-cell lysates were analyzed by Western blotting. (D) U2OS cells were transfected with the indicated siRNA oligonucleotides for 48 h prior to lysis. Whole-cell lysates (200 μg) were used to immunoprecipitate IκBα. Levels of RelA and IκBα present in the immunoprecipitates were analyzed by Western blotting and quantified using ImageJ software. (E) U2OS cells were transfected with a control siRNA or a Senp5 (S5a, S5b), Senp6 (S6a, S6b), or Senp7 (S7a, S7b) siRNA oligonucleotide, and total RNA was extracted. IL-8 and IAP2 mRNA levels were determined by qPCR. *, $P \leq 0.050$; **, $P \leq 0.010$. (F) U2OS cells were transfected with the indicated siRNA oligonucleotides for 48 h prior to lysis. Whole-cell lysates were analyzed by Western blotting. Levels of IAP2 were quantified using ImageJ software.

of HIF, are subsequently activated, in a cell/tissue-dependent manner, in prolonged hypoxia.

Our results indicate that IKK–NF-κB activation via the Ca^{2+}/CaMK2 pathway precedes the inhibition of the PHD oxygen molecular sensors and HIF-1α (Fig. 1 and 8). If the PHD enzymes were involved in the initial activation of the NF-κB pathway, their depletion should mimic the hypoxic stimulus and induce higher levels of activation. However, we could not detect any significant change in IKK activity in the absence of any of the PHD enzymes (Fig. 8). Furthermore, we could demonstrate that hypoxia-induced IKK-IκBα phosphorylation was HIF-1α independent. This independence of HIF-1α was also observed by An and colleagues (3). Our results, however, are in contrast with the previously suggested repression of IKK activity by PHD1 (9). Despite the IKKs' possessing the consensus for hydroxylation, LXLAP, this modification on IKK has not been formally demonstrated. We did not observe any effect of PHD1 depletion on IKK activity (Fig. 8). It is possible that the differences between the studies are due to technical reasons.

We have found that IKK activation following hypoxia requires TAK1; however, neither TAB1 nor TAB2 is essential (Fig. 7). It is possible that TAB3 can compensate for the lack of these other accessory proteins (6). A number of recent studies have shown that TAB1 is dispensable for TAK1 activation following treatment with a variety of stimuli (4, 26, 38). Our data suggest that CaMK2-mediated activation of TAK1 does not strictly require the TABs. Ubiquitination of Nemo/IKKγ or TRAFs can compensate for the lack of TAB1 in certain instances. Although we could not find a role for TRAF2 or TRAF6 in the activation of NF-κB, our studies demonstrate that Nemo/IKKγ and Ubc13 were essential for this effect (Fig. 6G and 11).

One of the more puzzling observations regarding hypoxia-induced NF-κB is the lack of IκBα degradation despite the phosphorylation by IKK. We determined that hypoxia prevented the ubiquitination of IκBα by a mechanism involving Sumo-2/3 conjugation (Fig. 12). Sumoylation of IκBα has been described for Sumo-1 conjugation, where it results in NF-κB inhibition (11). Our results indicate that Sumo-2/3 conjugation to IκBα results in activation. At present we cannot verify whether hypoxia induces Sumo-2/3 conjugation or prevents deconjugation by inhibition of Senps. Our data seem to point to the latter possibility, since depletion of Senps is sufficient to prevent IκBα degradation and activate NF-κB (Fig. 13). We have identified Senp5 to Senp7 as being particularly important for NF-κB activation (Fig. 13). We could not detect any change in the protein levels of these Senps (data not shown); however, at present it is not possible to determine changes in the activities of specific Senps. The biological functions of the Senps are only now being determined (20). Senp3, Senp5, Senp6, and Senp7 have been shown to preferentially deconjugate Sumo-2/3 over Sumo-1 *in vivo* (20). This is consistent with our data demonstrating increased levels of Sumo-2/3 conjugation on IκBα (Fig. 12). Furthermore, Sumo-2/3 can make Sumo chains both *in vitro* and *in vivo*, while Sumo-1 cannot (24, 37). Thus, conjugation of Sumo-2/3 chains on IκBα could be sufficient to induce the dissociation from RelA. This is consistent with our results finding that depletion of Senp3, Senp5, Senp6, and Senp7 is sufficient for RelA release (Fig. 13D). In the future, it will be interesting to investigate how specific Senps are regulated.

Our data demonstrate a novel and rapid activation of NF-κB in response to hypoxia and begin to elucidate how cells are able to initiate a rapid yet coordinated cellular response leading to the upregulation of survival factors, cooperation with other signaling pathways, and, ultimately, cellular survival.

ACKNOWLEDGMENTS

We are grateful to P. Cohen (Dundee, United Kingdom), M. Kracht (Hannover, Germany), V. Rangnekar (Lexington, KY), M. Ashcroft (London, United Kingdom), C. Bracken (Adelaide, Australia), I. Verma (San Diego, CA), S. Akira (Tokyo, Japan), S. Gosh (San Diego, CA), C. Smythe (Sheffield, United Kingdom), D. Ron (New York, NY), T. Mak (Toronto, Canada), M. Pasparakis (Cologne, Germany), and M. Soares (Oeiras, Portugal) for providing us with critical reagents. We are thankful to all members of the Rocha laboratory for comments on the manuscript. We are very grateful to R. Hay (Dundee, United Kingdom), P. Cohen (Dundee, United Kingdom), and N. Perkins (Newcastle, United Kingdom) for providing reagents and valuable comments.

This study was funded mainly by a New Investigator Research grant from the Medical Research Council (to C.C., S.M., and S.R.). S.R. is funded by a Research Council UK fellowship and the University of Dundee. A.M. is funded by a Wellcome Trust studentship. D.X. and A.S. were funded by a career development fellowship from the Association of International Cancer Research.

REFERENCES

1. **Adhikari, A., M. Xu, and Z. J. Chen.** 2007. Ubiquitin-mediated activation of TAK1 and IKK. Oncogene **26:**3214–3226.
2. **Aley, P. K., K. E. Porter, J. P. Boyle, P. J. Kemp, and C. Peers.** 2005. Hypoxic modulation of Ca^{2+} signaling in human venous endothelial cells. Multiple roles for reactive oxygen species. J. Biol. Chem. **280:**13349–13354.
3. **An, J., D. Mo, H. Liu, M. S. Veena, E. S. Srivatsan, R. Massoumi, and M. B. Rettig.** 2008. Inactivation of the CYLD deubiquitinase by HPV E6 mediates hypoxia-induced NF-κB activation. Cancer Cell **14:**394–407.
4. **Bertelsen, M., and A. Sanfridson.** 2007. TAB1 modulates IL-1α mediated cytokine secretion but is dispensable for TAK1 activation. Cell. Signal. **19:**646–657.
5. **Cai, H., D. Liu, and J. G. Garcia.** 2008. CaM kinase II-dependent pathophysiological signalling in endothelial cells. Cardiovasc. Res. **77:**30–34.
6. **Cheung, P. C., A. R. Nebreda, and P. Cohen.** 2004. TAB3, a new binding partner of the protein kinase TAK1. Biochem. J. **378:**27–34.
7. **Chin, E. R.** 2005. Role of Ca^{2+}/calmodulin-dependent kinases in skeletal muscle plasticity. J. Appl. Physiol. **99:**414–423.
8. **Courtois, G.** 2008. Tumor suppressor CYLD: negative regulation of NF-κB signaling and more. Cell. Mol. Life Sci. **65:**1123–1132.
9. **Cummins, E. P., E. Berra, K. M. Comerford, A. Ginouves, K. T. Fitzgerald, F. Seeballuck, C. Godson, J. E. Nielsen, P. Moynagh, J. Pouyssegur, and C. T. Taylor.** 2006. Prolyl hydroxylase-1 negatively regulates IκB kinase-β, giving insight into hypoxia-induced NF-κB activity. Proc. Natl. Acad. Sci. U. S. A. **103:**18154–18159.
10. **Cummins, E. P., and C. T. Taylor.** 2005. Hypoxia-responsive transcription factors. Pflugers Arch. **450:**363–371.
11. **Desterro, J. M., M. S. Rodriguez, and R. T. Hay.** 1998. SUMO-1 modification of IκBα inhibits NF-κB activation. Mol. Cell **2:**233–239.
12. **Droma, Y., T. Hayano, Y. Takabayashi, T. Koizumi, K. Kubo, T. Kobayashi, and M. Sekiguchi.** 1996. Endothelin-1 and interleukin-8 in high altitude pulmonary oedema. Eur. Respir. J. **9:**1947–1949.
13. **Fandrey, J., T. A. Gorr, and M. Gassmann.** 2006. Regulating cellular oxygen sensing by hydroxylation. Cardiovasc. Res. **71:**642–651.
14. **Garcia, J. A.** 2006. HIFing the brakes: therapeutic opportunities for treatment of human malignancies. Sci. STKE **2006:**pe25.
15. **Gilmore, T. D.** 2006. Introduction to NF-κB: players, pathways, perspectives. Oncogene **25:**6680–6684.
16. **Gilmore, T. D.** 1999. The Rel/NF-κB signal transduction pathway: introduction. Oncogene **18:**6842–6844.
17. **Kaelin, W. G., Jr., and P. J. Ratcliffe.** 2008. Oxygen sensing by metazoans: the central role of the HIF hydroxylase pathway. Mol. Cell **30:**393–402.
18. **Kenneth, N. S., S. Mudie, P. van Uden, and S. Rocha.** 2009. SWI/SNF regulates the cellular response to hypoxia. J. Biol. Chem. **284:**4123–4131.
19. **Kenneth, N. S., and S. Rocha.** 2008. Regulation of gene expression by hypoxia. Biochem. J. **414:**19–29.
20. **Kim, J. H., and S. H. Baek.** 2009. Emerging roles of desumoylating enzymes. Biochim. Biophys. Acta **1792:**155–162.

21. **Kim, K. S., V. Rajagopal, C. Gonsalves, C. Johnson, and V. K. Kalra.** 2006. A novel role of hypoxia-inducible factor in cobalt chloride- and hypoxia-mediated expression of IL-8 chemokine in human endothelial cells. J. Immunol. **177:**7211–7224.
22. **Koong, A. C., E. Y. Chen, and A. J. Giaccia.** 1994. Hypoxia causes the activation of nuclear factor κB through the phosphorylation of IκBα on tyrosine residues. Cancer Res. **54:**1425–1430.
23. **Kubo, K., M. Hanaoka, T. Hayano, T. Miyahara, T. Hachiya, M. Hayasaka, T. Koizumi, K. Fujimoto, T. Kobayashi, and T. Honda.** 1998. Inflammatory cytokines in BAL fluid and pulmonary hemodynamics in high-altitude pulmonary edema. Respir. Physiol. **111:**301–310.
24. **Lima, C. D., and D. Reverter.** 2008. Structure of the human SENP7 catalytic domain and poly-SUMO deconjugation activities for SENP6 and SENP7. J. Biol. Chem. **283:**32045–32055.
25. **Liu, X., M. Yao, N. Li, C. Wang, Y. Zheng, and X. Cao.** 2008. CaMKII promotes TLR-triggered proinflammatory cytokine and type I interferon production by directly binding and activating TAK1 and IRF3 in macrophages. Blood **112:**4961–4970.
26. **Mendoza, H., D. G. Campbell, K. Burness, J. Hastie, N. Ronkina, J. H. Shim, J. S. Arthur, R. J. Davis, M. Gaestel, G. L. Johnson, S. Ghosh, and P. Cohen.** 2008. Roles for TAB1 in regulating the IL-1-dependent phosphorylation of the TAB3 regulatory subunit and activity of the TAK1 complex. Biochem. J. **409:**711–722.
27. **Pahl, H. L.** 1999. Activators and target genes of Rel/NF-κB transcription factors. Oncogene **18:**6853–6866.
28. **Patitucci, M., D. Lugrin, and G. Pages.** 2009. Angiogenic/lymphangiogenic factors and adaptation to extreme altitudes during an expedition to Mount Everest. Acta Physiol. (Oxf.) **196:**259–265.
29. **Perkins, N. D.** 2000. The Rel/NF-κB family: friend and foe. Trends Biochem. Sci. **25:**434–440.
30. **Perkins, N. D., and T. D. Gilmore.** 2006. Good cop, bad cop: the different faces of NF-κB. Cell Death Differ. **13:**759–772.
31. **Rocha, S.** 2007. Gene regulation under low oxygen: holding your breath for transcription. Trends Biochem. Sci. **32:**389–397.
32. **Rocha, S., K. J. Campbell, and N. D. Perkins.** 2003. p53- and Mdm2-independent repression of NF-κB transactivation by the ARF tumor suppressor. Mol. Cell **12:**15–25.
33. **Rocha, S., M. D. Garrett, K. J. Campbell, K. Schumm, and N. D. Perkins.** 2005. Regulation of NF-κB and p53 through activation of ATR and Chk1 by the ARF tumour suppressor. EMBO J. **24:**1157–1169.
34. **Sato, S., H. Sanjo, K. Takeda, J. Ninomiya-Tsuji, M. Yamamoto, T. Kawai, K. Matsumoto, O. Takeuchi, and S. Akira.** 2005. Essential function for the kinase TAK1 in innate and adaptive immune responses. Nat. Immunol. **6:**1087–1095.
35. **Scheidereit, C.** 2006. IκB kinase complexes: gateways to NF-κB activation and transcription. Oncogene **25:**6685–6705.
36. **Semenza, G. L.** 2008. Hypoxia-inducible factor 1 and cancer pathogenesis. IUBMB Life **60:**591–597.
37. **Shen, L. N., M. C. Geoffroy, E. G. Jaffray, and R. T. Hay.** 2009. Characterization of SENP7, a SUMO-2/3-specific isopeptidase. Biochem. J. **421:**223–230.
38. **Shim, J. H., C. Xiao, A. E. Paschal, S. T. Bailey, P. Rao, M. S. Hayden, K. Y. Lee, C. Bussey, M. Steckel, N. Tanaka, G. Yamada, S. Akira, K. Matsumoto, and S. Ghosh.** 2005. TAK1, but not TAB1 or TAB2, plays an essential role in multiple signaling pathways in vivo. Genes Dev. **19:**2668–2681.
39. **Terzic, J., I. Marinovic-Terzic, F. Ikeda, and I. Dikic.** 2007. Ubiquitin signals in the NF-κB pathway. Biochem. Soc. Trans. **35:**942–945.
40. **Toescu, E. C.** 2004. Hypoxia sensing and pathways of cytosolic Ca^{2+} increases. Cell Calcium **36:**187–199.
41. **Tokunaga, F., S. Sakata, Y. Saeki, Y. Satomi, T. Kirisako, K. Kamei, T. Nakagawa, M. Kato, S. Murata, S. Yamaoka, M. Yamamoto, S. Akira, T. Takao, K. Tanaka, and K. Iwai.** 2009. Involvement of linear polyubiquitylation of NEMO in NF-κB activation. Nat. Cell Biol. **11:**123–132.
42. **Xirodimas, D. P., A. Sundqvist, A. Nakamura, L. Shen, C. Botting, and R. T. Hay.** 2008. Ribosomal proteins are targets for the NEDD8 pathway. EMBO Rep. **9:**280–286.